Université du Québec
Institut National de la Recherche Scientifique
Centre Eau Terre Environnement

DÉVELOPPEMENT D'UNE MÉTHODE DE CARACTÉRISATION DE L'ÉTAT DE BANDES RIVERAINES EN MILIEU AGRICOLE À L'AIDE DE LA TÉLÉDÉTECTION SATELLITAIRE À TRÈS HAUTE RÉSOLUTION SPATIALE

Par

Julio Novoa

Mémoire présentée pour l'obtention du grade de
Maître ès sciences (M.Sc.)
en sciences de l'eau

Jury d'évaluation

Examinateur interne	Alain N. Rousseau INRS Centre Eau Terre Environnement
Examinateur externe	Jacques Gallichand Faculté des sciences de l'agriculture et de l'alimentation Université Laval
Directeur de recherche	Karem Chokmani INRS Centre Eau Terre Environnement
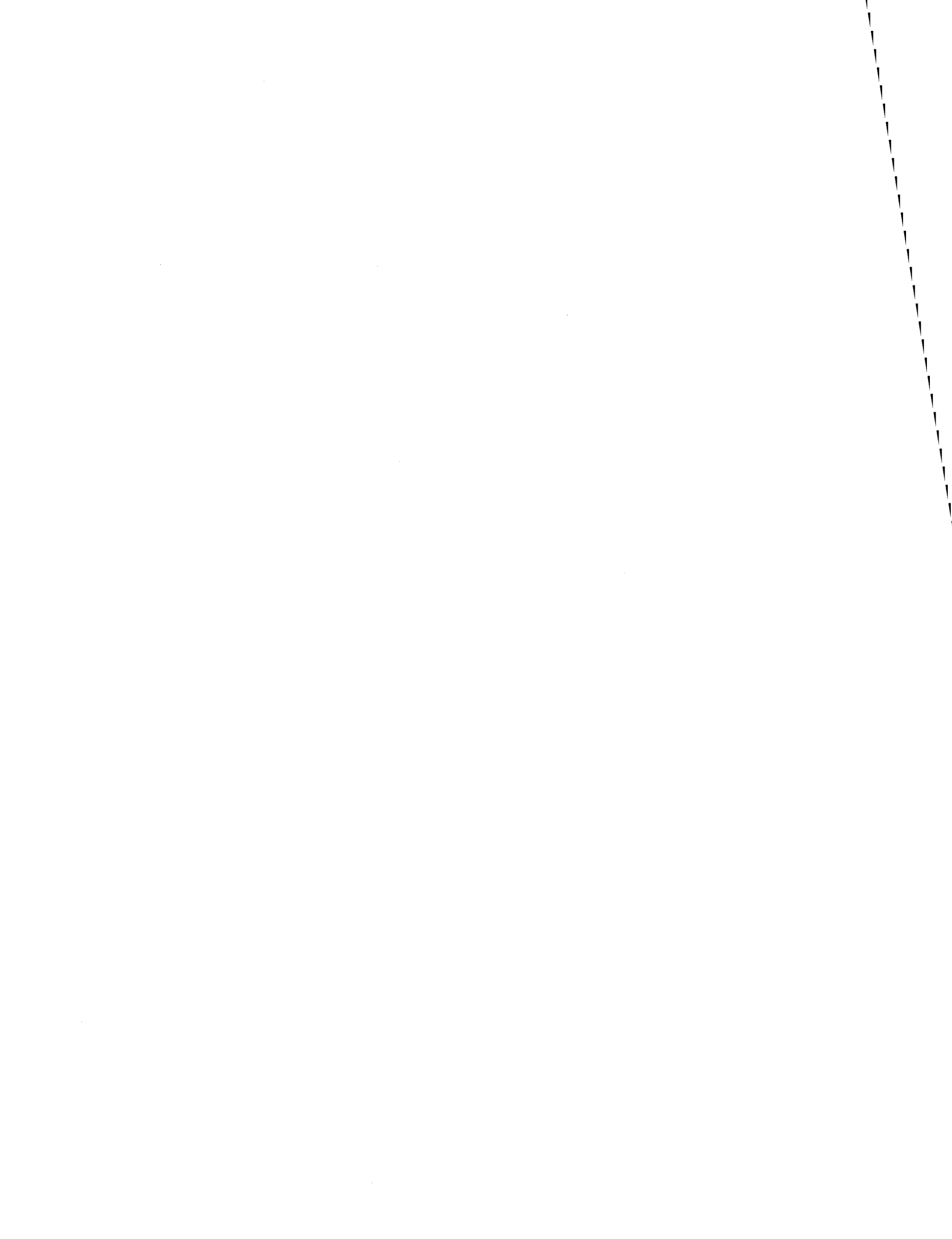
Je dédie ce travail à mon épouse Milena, et à mes filles Maria-Eduarda, Maria-Victoria et Isabella, sans qui rien n'aurait été possible.

REMERCIEMENTS

Je tiens à remercier mon directeur de recherche Professeur Karem Chokmani de m'avoir accueilli dans son équipe. Sa patience et son soutien ont été précieux afin de mener mon travail à bon port. Je voudrais remercier les organismes CAPSA et MAPAQ pour la confiance déposée sur moi et pour les soutiens logistique et financier. Mes remerciements vont aussi à toute l'équipe du Laboratoire de Télédétection qui m'a encouragé tout au long de ce travail. Enfin, je voudrais aussi remercier les reviseurs de ce mémoire pour leur travail acharné, et tous les professeurs de l'INRS pour leur aide inconditionnelle pendant mon séjour à Québec.

RÉSUMÉ

Les bandes riveraines figurent de plus en plus parmi les solutions envisagées pour protéger la qualité des eaux. La condition écologique de cet habitat riverain est évaluée au Québec à l'aide de l'indice de qualité de la bande riveraine. Les techniques utilisées actuellement demeurent très exigeantes quant aux ressources matérielles et humaines, par conséquent, il est nécessaire de développer des approches opérationnelles non seulement pour évaluer sa qualité écologique, mais aussi pour évaluer son efficacité à filtrer les eaux de ruissellement en milieu agricole. Ainsi, la télédétection à très haute résolution spatiale s'avère une alternative efficace car elle peut fournir en même temps de l'information altitudinale et spectrale. Par conséquent, un modèle numérique du terrain, extrait à partir des images satellitaires stéréoscopiques, a été évalué sur trois champs agricoles. Les résultats montrent que le modèle satellitaire a été capable de bien représenter l'altitude au niveau global, mais il a eu de la difficulté à représenter la microtopographie intra-parcellaire, notamment en terrain plat. En ce qui concerne l'extraction de la couverture végétale riveraine, l'information spectrale satellitaire a permis de produire une carte de végétation avec un niveau de précision global très satisfaisant (indice de kappa de 0,82). Les résultats montrent que l'indice de qualité de la bande riveraine obtenu par méthode satellitaire proposée est conforme à l'indice obtenu à partir d'observations in-situ. De plus, un indice d'efficacité de la bande riveraine par rapport à sa capacité à intercepter les eaux de ruissellement des parcelles agricoles adjacentes, a été développé. Ceci inclue une mesure de la qualité du drainage qui vise mesurer le degré de concentration des eaux d'écoulement dans les bandes riveraines. Avec cet indice proposé, les bandes riveraines les moins efficaces sont facilement identifiées, ce qui contribue ultimement à une meilleure gestion de l'environnement en milieu riveraine et agricole.

ABSTRACT

Riparian strips have been recognized as one of the solutions to protect water quality. In Quebec, the ecological condition of the riparian habitat is assessed using a riparian strip quality index. Current techniques are very demanding in terms of human and material resources, therefore, it is necessary to develop operational approaches not only to assess its ecological quality, but also to assess its effectiveness in filtering runoff in agricultural areas. Thus, remote sensing at very high spatial resolution appears as a less expensive alternative because it can provide, at the same time, altitudinal and spectral information. Therefore, a digital elevation model extracted from stereoscopic satellite imagery was evaluated on three agricultural fields. The results show that, overall, the satellite model was able to accurately represent the altitude, but it had problems when depicting the microtopography, especially in flat terrain. Regarding the extraction of riparian vegetation, the satellite spectral information allowed to produce a vegetation map with a very satisfactory overall accuracy (kappa = 0.82). The results show that the riparian strip quality index obtained by the proposed satellite method is consistent with the index obtained from in-situ observations. In addition, a riparian strip efficiency index relative to its ability to intercept runoff from contiguous agricultural fields, has been developed. This includes a measure of the drainage quality which aims to measure the degree of concentration of runoff in riparian zones. With this proposed index, the least effective riparian strips are easily identified, which ultimately contributes to improve the environmental management in riparian and agricultural areas.

TABLE DES MATIÈRES

LISTE DES TABLEAUX

LISTE DES FIGURES

DÉVELOPPEMENT D'UNE MÉTHODE DE CARACTÉRISATION DE L'ÉTAT DE BANDES RIVERAINES EN MILIEU AGRICOLE À L'AIDE DE LA TÉLÉDÉTECTION SATELLITAIRE À TRÈS HAUTE RÉSOLUTION SPATIALE

SYNTHÈSE

1 INTRODUCTION

1.1 Contexte

Les bandes riveraines sont considérées comme l'une des pratiques environnementales les plus efficaces pour protéger la qualité des eaux. Ainsi, dans les zones agricoles - grâce à leur capacité filtrante – les bandes riveraines sont mise en place pour contribuer à réduire la pollution diffuse en retenant les sédiments, les nutriments et les pesticides transportés par les eaux de ruissellement (Borin *et al.*, 2010, Duchemin *et al.*, 2004, Lowrance *et al.*, 1997, Sahu *et al.*, 2009). Les bandes riveraines ont également d'autres fonctions écologiques, incluant le contrôle de l'érosion induit par le système racinaire de la végétation riveraine pour augmenter la rugosité du terrain et favoriser l'infiltration (Vought *et al.*, 1995), comme une source de nourriture pour les espèces terrestres et aquatiques (Naiman *et al.*, 1997), et pour le contrôle de la température de l'eau (Janisch *et al.*, 2012). En plus de ces fonctions écologiques, d'assainissement et de protection, les bandes riveraines contribuent aussi à l'intégrité et l'esthétisme du paysage rural. Dans l'est du Canada, où la production agricole est intensive, elles jouent un rôle essentiel dans la protection de l'environnement (Boutin *et al.*, 2003).

1.2 Problématique

Au Québec, la condition écologique des habitats riverains est évaluée à l'aide de l'indice de qualité de la bande riveraine (IQBR). Cet indice est basé sur la superficie relative occupée par neuf composantes de l'utilisation du sol en milieu riverain : forêt, arbustive, herbacée naturelle, cultures, friche/fourrage/pâturage/pelouse, coupe forestière, sol nu, socle rocheux et infrastructure (Mddefp, 2008). L'IQBR est un outil primordial pour les organismes de gestion des bassins versants, qui sont les acteurs principaux dans la gestion intégrée de l'eau. Ces organismes ont le mandat d'élaborer un plan directeur de l'eau incluant un portrait général du bassin versant et les solutions envisagées pour mieux le gérer. Pour ce faire, les techniques traditionnelles de cartographie se basent essentiellement sur les observations sur le terrain assistées par la photographie aérienne. À titre d'exemple, le Groupe de concertation du bassin versant de la rivière Bécancour a réalisé en 2006 un portrait global des bandes riveraines sur une portion de la rivière Bécancour à l'aide de relevés de terrain réalisés en canot. Les résultats ont été compilés dans un SIG et ont permis de cartographier le type de végétation et l'état des

3

bandes riveraines (Chauvette, 2006). Ces techniques demeurent toutefois très subjectives et à la fois exigeantes en termes de ressources matérielles et humaines et ne permettent pas de couvrir de grandes superficies, sans être pour autant précises en raison de la vue partielle que l'on a de l'utilisation du sol riveraine. Par conséquent, il est nécessaire de développer des approches opérationnelles, non seulement pour cartographier le couvert végétal dans les zones riveraines, mais aussi pour évaluer sa qualité et son efficacité, surveiller les changements qui y surviennent, identifier les zones à prioriser pour des activités de restauration ainsi que d'évaluer le succès des mesures de gestion antérieures (Goetz, 2006). Toutefois, la cartographie précise des écosystèmes riverains constitue un réel défi étant donné la nature complexe de ces milieux (Gergel *et al.*, 2007).

L'utilisation de la télédétection pour cartographier les bandes riveraines n'est pas une pratique récente. Elle a été popularisé avec la photographie aérienne, principalement à cause de sa bonne résolution spatiale et aussi comme une alternative viable aux campagnes de terrain coûteuses (Goetz, 2006, Muller *et al.*, 1993). Toutefois, cette méthode pour cartographier la végétation riveraine offre une résolution spectrale limitée et nécessite plusieurs traitements additionnels tels que la numérisation, l'orthorectification, le mosaïquage et la photo-interprétation, contribuant ainsi à augmenter les coûts de production sur les grandes étendues et limitant les possibilités de mises à jour plus fréquentes (Gergel *et al.*, 2007, Yang, 2007b). L'imagerie satellitaire à moyenne résolution spatiale (taille du pixel entre 4 et 30 m), dans ses débuts avec moins de résolution spatiale que la photographie aérienne, continue d'être utilisée telle que dans la caractérisation et le suivi de l'état des milieux riverains aux États-Unis (Jones *et al.*, 2010) ou pour le suivi de la dynamique spatiale de l'activité agricole en bordure des rivières au Canada (Gu *et al.*, 2010).

Les progrès récents en matière de télédétection satellitaire, en particulier l'avènement de l'imagerie satellitaire à très haute résolution spatiale (taille du pixel de moins de 1 m), ont amélioré sensiblement le potentiel de ces technologies pour le suivi et la gestion des bandes riveraines à des échelles locales (Ashraf *et al.*, 2010) et ce, à des coûts d'acquisition par hectare très avantageux, évalués à 0,30$/ha pour les données satellitaires versus la photo aérienne estimée à 1,22$/ha (Vézina *et al.*, 2003).

Aujourd'hui, un certain nombre de satellites commerciaux (WorldView, GeoEye, Pléiades) sont capables d'acquérir des images multispectrales à une résolution spatiale inférieure à 2 m et des données panchromatiques à moins de 50 cm de résolution matricielle, s'approchant ainsi du niveau de détail de la photographie aérienne. Toutefois, étant donné que l'imagerie satellitaire à

4

très haute résolution spatiale implique une très grande hétérogénéité dans l'information spectrale disponible à traiter, les techniques usuelles de traitement d'image pixel à pixel peuvent s'avérer insuffisantes et risquent de produire des résultats peu cohérents (Johansen *et al.*, 2010). En effet, l'approche orientée-objet s'est avérée très efficace pour extraire l'information à partir de l'imagerie satellitaire à très haute résolution spatiale en vue de caractériser des bandes riveraines (Johansen *et al.*, 2007). La classification orientée-objet utilise non seulement l'information spectrale des objets homogènes identifiés dans l'image mais aussi les informations spatiale, géométrique, sémantique et topologique des objets identifiés. Elle permet également de hiérarchiser le processus de classification en différents niveaux sémantiques pour mieux gérer l'extraction d'information spatiale (Blaschke, 2010). De plus, elle permet d'intégrer toute couche d'information auxiliaire à l'imagerie satellitaire, ce qui s'avère très utile pour la cartographie d'un environnement aussi complexe que les zones riveraines. Au Québec, aucune étude appliquée à la problématique de suivi et de gestion des bandes riveraines et combinant l'imagerie à très haute résolution spatiale et la classification orientée-objet n'a été recensée pendant la réalisation du présent projet de recherche.

Par ailleurs, les modèles numériques du terrain sont largement utilisés pour la simulation des processus de surface, spécialement dans la modélisation hydrologique des bassin versants (Burrough, 1986, Jacobsen, 2004, Li *et al.*, 2005, Moore *et al.*, 1991). Cette source d'information spatiale permet également de générer plusieurs variables reliées à l'écoulement de surface au niveau des parcelles (Devenecia *et al.*, 2007, Lyon *et al.*, 2003, Nardi *et al.*, 2008). Ainsi, la pente du terrain, les directions d'écoulement, les limites des micro-bassins, la concentration d'écoulement et la localisation des exutoires sont des variables complémentaires à l'imagerie à très haute résolution spatiale et indispensables pour caractériser les bandes riveraines en termes de qualité écologique et d'efficacité à intercepter des eaux de ruissellement en milieu agricole (Hickey *et al.*, 2004, Hupp *et al.*, 1996). À ce titre, le satellite WorldView-2 s'avère une source de données idéale puisqu'il offre à la fois, de l'information multispectrale avec huit bandes spectrales et de l'information altimétrique avec un modèle numérique de terrain. Cette information servira pour l'extraction d'information sur l'utilisation du sol et des paramètres géomorphologiques et de drainage, qui serviront ultérieurement à l'évaluation de la qualité et l'efficacité écologique des bandes riveraines.

1.3 Objectifs de recherche

L'objectif de ce projet de recherche est de développer une méthode opérationnelle pour la caractérisation des bandes riveraines à l'aide de l'imagerie satellitaire à très haute résolution spatiale et de la classification orientée-objet. Pour ce faire, deux volets séquentiels ont été définis : (1) évaluer la qualité du modèle numérique du terrain satellitaire à représenter la microtopographie en milieu agricole, et (2) développer une méthodologie pour évaluer la qualité et l'efficacité des bandes riveraines à l'aide de l'information satellitaire multispectrale et altimétrique.

2 MÉTHODES

2.1 Zone d'étude

Le bassin versant de La Chevrotière est localisé dans la municipalité de Portneuf, 60 km à l'ouest de la ville de Québec. La rivière La Chevrotière est un tributaire direct du fleuve Saint-Laurent. Elle s'écoule sur 29 km. Son bassin versant, qui est caractérisé par un relief de plat à vallonné, totalise une superficie de 108 km². Les zones riveraines du cours d'eau sont couvertes majoritairement de forêts et de zones de pâturages et cultures. Comme la plupart des bassins versants avec des activités agricoles intensives, le bassin versant de La Chevrotière fait face aux problématiques liées à la pollution diffuse, à l'érosion des berges et à la dégradation des sols agricoles (Figure 2.1).
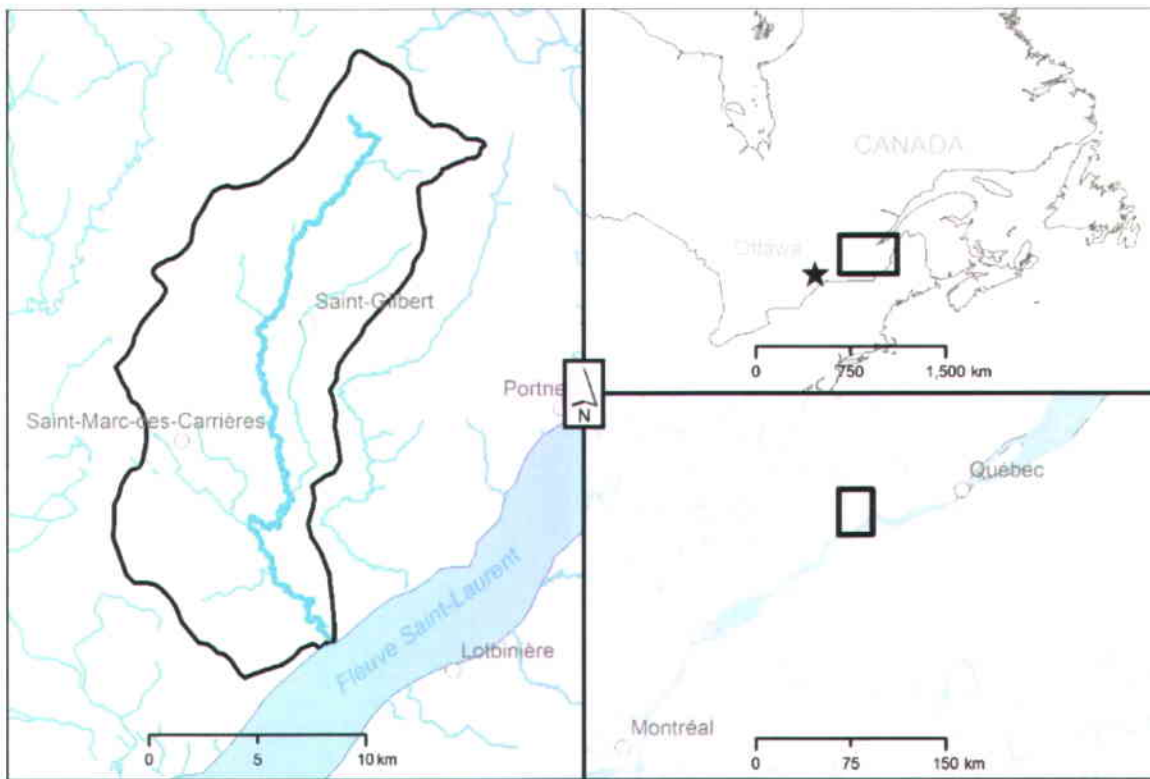
Figure 2.1 : Localisation du bassin versant de la rivière La Chevrotière.

2.2 Données

Deux jeux de données ont été utilisés dans le présent projet : (1) les relevés terrain, composés de l'information GPS acquise avec la méthode cinématique en temps réel (GPS-RTK), ainsi que des observations sur l'utilisation du sol dans les zones riveraines d'étude, et (2) les données satellitaires, composées de deux images multispectrales, ainsi que d'un MNT extrait par stéréoscopie à partir de l'imagerie satellitaire. Plus de détails sur ces jeux de données sont présentés au Tableau 2.1.

Tableau 2.1 : Description de données utilisées.

Données géospatiales		Détails
Relevés terrain	Points GPS-RTK	~130 000 points relevés dans trois champs agricoles Précision horizontale/verticale : ±0,1 m
	Échantillons utilisation du sol	80 échantillons (segments de cours d'eau)
Imagerie satellitaire	Images multispectrales	2 images : été 2011, printemps 2012 8 bandes multispectrales (résolution spatiale : 2,0 m) 1 bande panchromatique (résolution spatiale : 0,5 m)
	Modèle numérique du terrain (MNT)	Source : image stéréoscopique du printemps 2012 Résolution horizontale : 1 m Précision verticale : 1 m

2.3 Approche méthodologique

L'approche méthodologique pour caractériser les bandes riveraines à l'aide de l'imagerie satellitaire à très haute résolution spatiale est résumée à la Figure 2.2, ci-dessous :
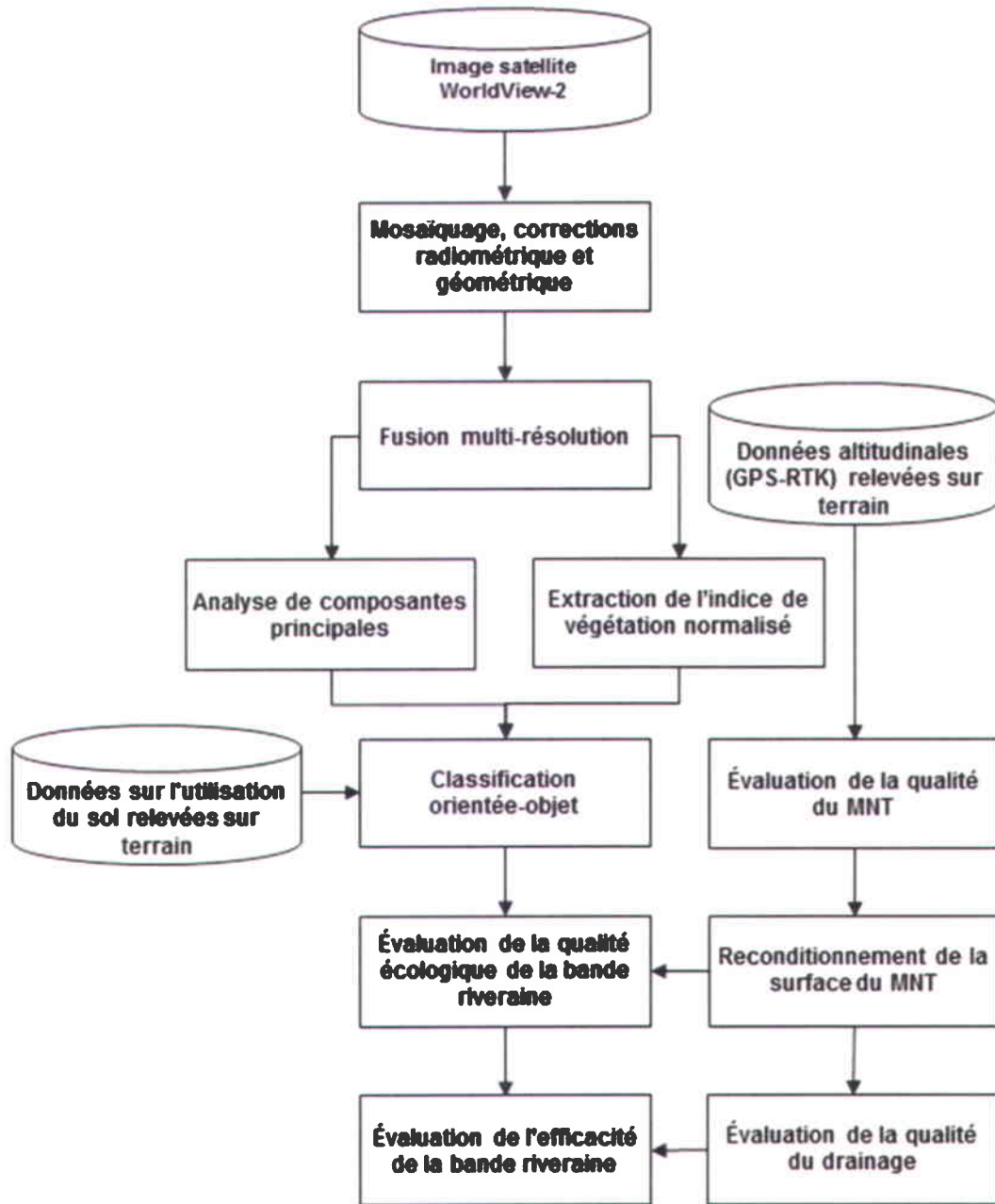
Figure 2.2 : Méthodologique pour caractériser les bandes riveraines à l'aide de la télédétection à très haute résolution spatiale.

2.3.1 Prétraitements des images satellitaires

L'information satellitaire doit subir une série de prétraitements séquentiels avant d'être utilisées. Étant donné que les images du satellite WorldView-2 sont souvent livrées sous forme de tuiles (sous-images) à cause de la très grande taille des fichiers en raison de leur très haute résolution spatiale, le premier prétraitement est le mosaïquage. Ceci consiste à mettre ensemble toutes les tuiles pour créer un seul fichier par image satellitaire. Par la suite, afin réduire les effets négatifs de l'atmosphère sur l'information spectrale captée par le satellite, une correction atmosphérique est appliquée aux images. Cette correction permet obtenir les vraies valeurs de réflectance de la surface de la Terre et ainsi améliorer la classification numérique des images satellitaires. Ensuite, les images sont ortho-rectifiées, c'est-à-dire, elles sont corrigées géométriquement afin de s'assurer que la position horizontale soit concordante entre tous les jeux de données. De plus, pour tirer profit des capacités de détection offertes par l'information des bandes multispectrales tout en bénéficiant de la très haute résolution spatiale de la bande panchromatique, une fusion multirésolution est appliquée. Ainsi, les huit bandes sont fusionnées avec la bande panchromatique afin de produire une image multispectrale à très haute résolution spatiale (taille du pixel = 0,5 m). Quant à la classification orientée-objet, l'information multispectrale de chaque image a été réduite de huit à deux bandes seulement : la première composante de l'analyse par composante principale et la deuxième étant l'indice de végétation normalisé. Ces deux bandes permettent de maximiser le contenu informationnel tout en réduisant le temps de calcul.

2.3.2 Évaluation de la qualité du modèle numérique de terrain satellitaire

Le modèle numérique de terrain produit par stéréoscopie satellitaire a été évalué selon sa capacité à : (a) représenter fidèlement l'altitude sur les parcelles agricoles, et (b) produire des variables géomorphologiques et du drainage, tels que la pente, les dépressions du terrain, l'accumulation d'écoulement de surface et l'emplacement des points de drainage riverains (Figure 2.3).

(a) Validation verticale

Comparaison entre le MNT satellitaire et les valeurs d'altitude des points GPS-RTK

↓

Évaluation des erreurs verticales

↓

Correction du biais d'élévation

(b) Validation hydrologique

Création des MNT à partir des points GPS-RTK

↓

Extraction des variables topographiques au niveau parcellaire

↓

Extraction des variables hydrologiques au niveau parcellaire

↓

Analyse comparative et évaluation des erreurs

Figure 2.3 : Validation (a) verticale (altimétrique) et (b) hydrologique du MNT satellitaire.

L'évaluation verticale du MNT s'est basée sur une comparaison entre le modèle satellitaire et ~130 000 points GPS à très haute précision (± 0,1 m) relevés sur le terrain dans trois champs agricoles de différentes caractéristiques topographiques. Cette étude a été faite pour s'assurer que les analyses postérieures sur la capacité des bandes riveraines à intercepter des eaux de ruissellement soient les plus fidèles que possible à la réalité. En conséquence, l'erreur linéaire au percentile 90e (LE90) et la précision verticale (Az) à un niveau de confiance de 95% ont été calculées (Ndep, 2004). L'erreur LE90 indique que 90% des erreurs des points mesurés ont des valeurs absolues égale ou moindre que LE90, et 10% des erreurs des points mesurés seront de plus grande valeur. La précision verticale, valide à condition que les erreurs mesurées suivent une distribution normale, est calculée comme suit :

$$Az = 1.96 * RMSEz \qquad (2.1)$$

où $RMSEz$ est l'erreur verticale quadratique moyenne.

Ensuite, l'évaluation de la capacité du MNT à représenter les processus d'écoulement de surface a été faite à l'aide des trois variables principales : (1) les dépressions du terrain, (2) la pente, et (3) les voies d'écoulement. Pour ce faire, un modèle numérique du terrain, avec la même taille de pixel que le MNT satellitaire, a été créé à partir des points GPS-RTK à très haute précision. Les erreurs ont été calculées de façon relative et exprimées en pourcentage pour faciliter la comparaison et la compréhension.

2.3.3 Évaluation de la qualité et l'efficacité des bandes riveraines

À partir des travaux de Saint-Jacques *et al.* (1998), le Ministère du Développement durable, de l'Environnement, de la Faune et des Parcs (MDDEFP) a développé un protocole de caractérisation de la bande riveraine (Mddefp, 2008). Ce protocole permet de collecter, *in situ*, l'information sur neuf composantes d'utilisation du sol requis pour évaluer la qualité écologique de la bande riveraine. Chacune de ces composantes a un facteur de pondération lui étant associé : (i) *végétation arborescente* (10), (ii) *végétation arbustive* (8,2), (iii) *végétation herbacée naturelle* (5,8), (iv) *coupe forestière* (4,3), (v) *socle rocheux* (3,8), (vi) *friche/fourrage/pâturage/pelouse* (3), (vii) *cultures* (1,9), (viii) *infrastructure* (1,9), et (ix) *sol nu* (1,7). L'IQBR, dont la valeur oscille entre 17 (très faible) et 100 (bon), est évalué à l'aide la formule suivante :

$$IQBR = \sum(d_i \times P_i) / 10 \qquad\qquad (2.2)$$

où i est la nième composante (ex. végétation arborescente, cultures, etc.), d est le pourcentage du secteur couvert par la composante i, P est le facteur de pondération de la composante i.

Le protocole technique du MDDEFP pour évaluer la qualité écologique des bandes riveraines à travers le calcul de l'IQBR consiste à recueillir des observations sur l'utilisation du sol dans des secteurs de rivière de 500 m de longueur. La méthodologie proposée pour évaluer la qualité de bandes riveraines à l'aide de l'imagerie satellitaire à très haute résolution spatiale utilise le même protocole technique, sauf dans les zones agricoles où la longueur des secteurs de rivière est concordante avec les limites des parcelles agricoles, c'est-à-dire, les secteurs sont de longueur variable. Pour ce faire, la classification orientée-objet a été appliquée car elle permet de baser nos analyses non seulement sur les valeurs spectrales des pixels, mais aussi sur des paramètres morphologiques et topologiques comme la taille, la forme et le voisinage des objets, ce qui améliore considérablement la qualité de l'information extraite des images à très haute

résolution spatiale (Blaschke, 2010). Ainsi, la méthode pour classifier les images satellitaires est décrite à la Figure 2.4, ci-dessous :
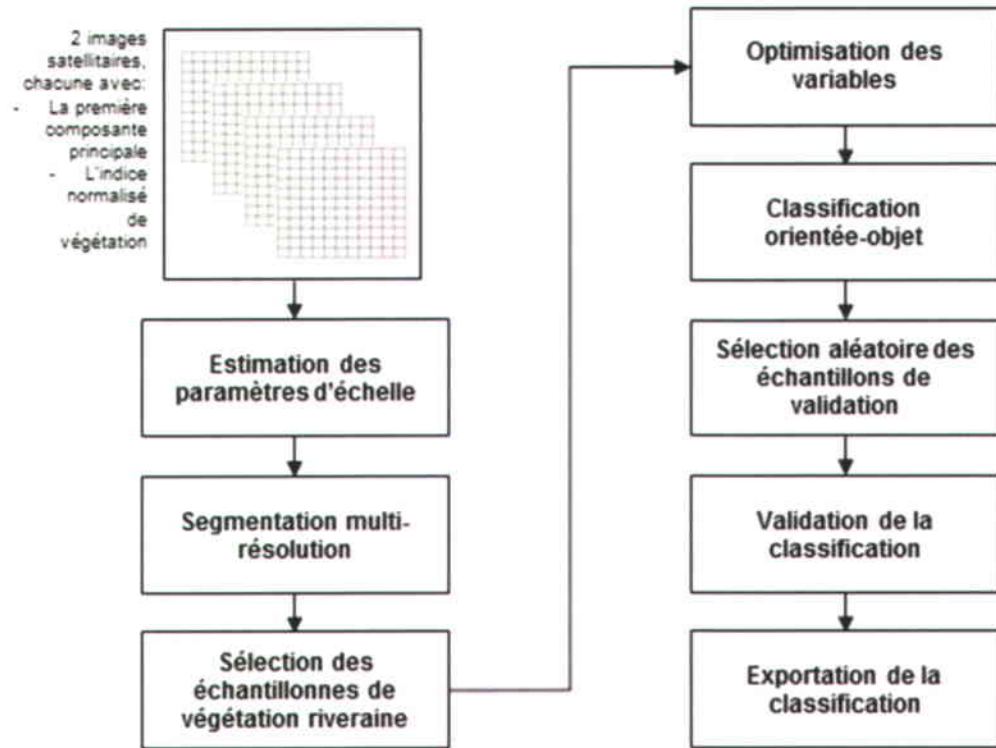
Figure 2.4 : Flux des processus de la classification orientée-objet.

Pour l'implantation de la classification orientée-objet, un jeu de données matricielles a été utilisé. Il est composé par quatre bandes spectrales : les premières composantes principales et les indices normalisés de végétation de deux images satellitaires 2011 et 2012. Ainsi, la première étape a été l'estimation de l'échelle de segmentation. Cette dernière définit la quantité, la taille et la forme des objets segmentés. Pour ce faire, le module ESP (Dragut *et al.*, 2010) a été utilisé pour déterminer d'une manière itérative les valeurs optimales de l'échelle de segmentation. Ce module analyse la variance spectrale locale des objets et le taux de changement de la quantité des objets crée entre deux échelles consécutives. Ainsi, à la Figure 2.5, on peut constater deux pics qui correspondent aux échelles de segmentation où les changements dans la quantité des objets sont significatifs (25 et 38). Après une vérification visuelle, l'échelle 25 a été choisie car elle était plus cohérente dans la quantité et la taille des objets créés.
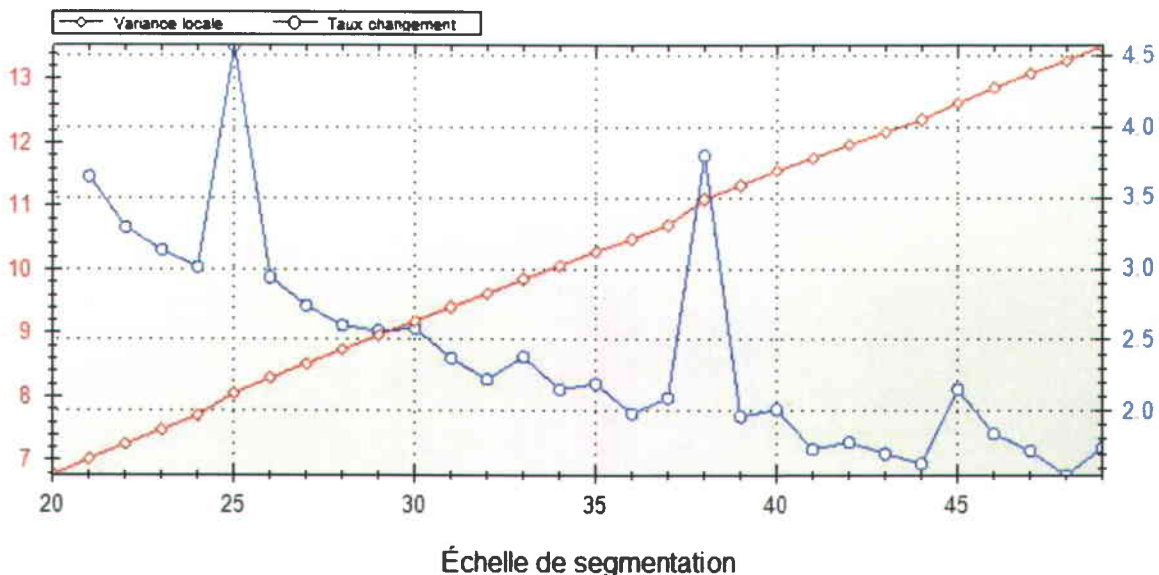
Figure 2.5 : Optimisation de l'échelle pour la segmentation multirésolution.

Une fois connue, l'échelle optimale de segmentation a permis de créer des objets homogènes (basés sur sa couleur et sa forme) avec l'image d'entrée. Ces objets ont été utilisés par la suite pour classifier l'image satellitaire à partir de l'information spectrale, de la texture, la géométrie et la topologie et ainsi produire la carte de végétation du bassin versant d'étude. Pour ce faire, une légende d'utilisation du sol, basée sur la formule du calcul de l'IQBR, a été créée et plusieurs objets ont été sélectionnés en tant qu'échantillons de végétation.

Étant donné que les images satellitaires présentent une très haute résolution spatiale qui permet de visualiser clairement les différents types de végétation dans la zone d'étude, la sélection des échantillons de végétation a été faite manuellement sur l'écran. Postérieurement, ces échantillons ont été évalués afin d'optimiser les variables pour la classification. Seize variables optimales ont été choisi par le logiciel : quatre variables morphologiques (superficie, luminosité, asymétrie spectrale, facteur de forme) par objet, trois variables statistiques (moyenne spectrale, écart-type spectral, différence spectrale maximale) par objet et pour chacune des quatre bandes spectrales. Ce processus itératif d'optimisation analyse la meilleure combinaison de variables pour mieux discriminer les objets qui seront attribuées aux catégories d'utilisation du sol.

Par la suite, une fois le jeu de variables optimales connu, l'algorithme du plus proche voisin (*Nearest Neighbor*) a été sélectionné pour classifier l'image satellitaire. Cet algorithme utilise la logique floue pour attribuer des objets à chacune des catégories de la légende d'utilisation du

14

sol. Dans cette logique, chaque objet est attribué à une catégorie de la légende selon son degré d'appartenance, c'est-à-dire selon la similitude statistique de l'ensemble d'échantillons de chaque catégorie. Un des avantages de cet algorithme est qu'il permet la réutilisation de cette méthode orientée-objet avec d'autres types d'images satellitaires à très haute résolution spatiale sans aucune modification. C'est ainsi qu'a été produit la carte de végétation.

Cette carte de végétation a été validée avec des échantillons (objets) choisis aléatoirement sur l'écran pour chacune des catégories d'utilisation du sol. Cette validation ayant pour objectif de comparer la coïncidence spatiale entre les échantillons de validation et les catégories d'utilisation du sol de la carte (Éq. 2.3). Comme résultat, une matrice de confusion a été générée, qui définit la précision globale de la classification numérique en utilisant l'indice de concordance kappa *K* (Congalton, 1991). Cet indice est évalué à l'aide la formule suivante :

$$K = \frac{N \sum_{i=1}^{r} x_{ii} - \sum_{i=1}^{r}(x_{i+} * x_{+i})}{N^2 - \sum_{i=1}^{r}(x_{i+} * x_{+i})}$$

(2.3)

où *r* est le nombre de lignes dans la matrice, X_{ii} est le nombre d'observations dans la ligne *i* et la colonne *i*, X_{i+} et X_{+i} sont les totaux marginaux de la ligne *i* et la colonne *i*, respectivement, et N est le nombre total d'observations.

Enfin, les résultats de la classification orientée-objet ont été exportés vers un format vectoriel et intégrés dans un système d'information géographique pour utilisation dans les traitements subséquents de l'analyse de la qualité et l'efficacité de la bande riveraine. La Figure 2.6 présente la méthode.
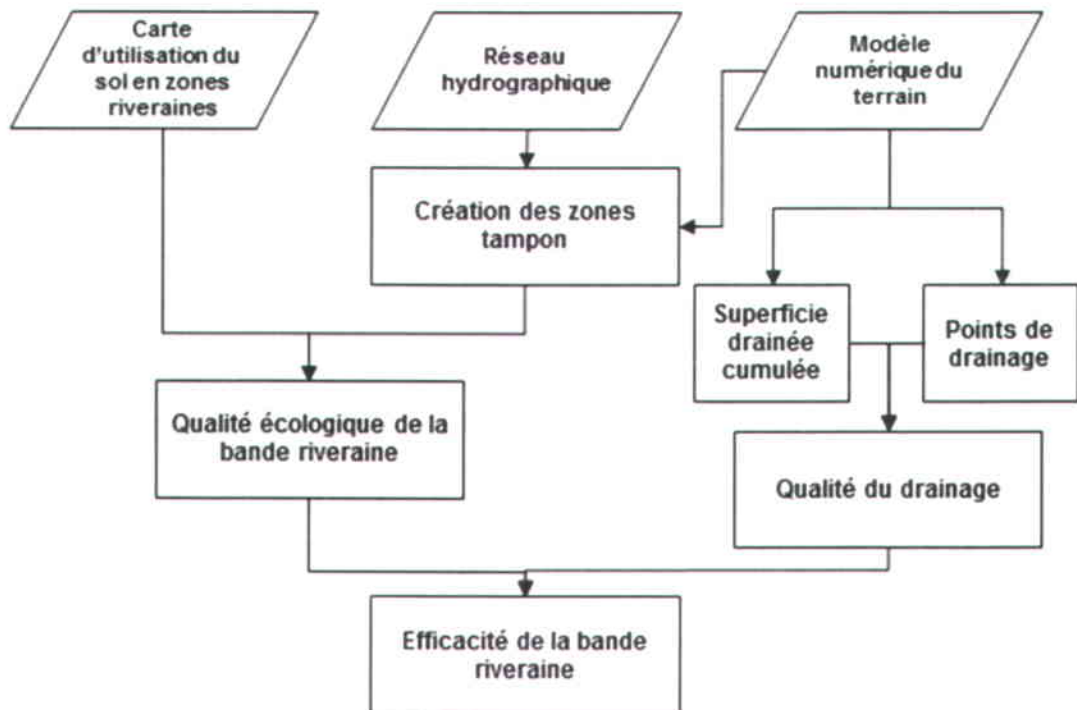
Figure 2.6 : Analyse de la qualité et l'efficacité de la bande riveraine.

Les méthodes d'analyse de la qualité et l'efficacité des bandes riveraines ont été mise en application à l'aide du logiciel ArcGIS. Il s'agit d'une approche semi-automatique qui nécessite trois données d'entrée : la carte d'utilisation du sol en zones riveraines (vecteur de polygones, résultat de la classification orientée-objet), le réseau hydrographique (vecteur de lignes) et le MNT satellitaire validé (voir Section 2.3.2). Tout d'abord, à partir du MNT et du réseau hydrographique, des zones tampon autour des cours d'eau ont été créées afin d'extraire l'information sur la couverture végétale des zones riveraines. Il faut noter que, selon la réglementation officielle provinciale, la largeur de ces zones tampon dépend du zonage du territoire et de la pente de la rive (Québec, 2005). Par exemple, en zone agricole, il faut respecter une largeur de 3 m sur les rives lorsque la pente est inférieure à 30%, tandis que si la pente est supérieure à 30%, il faut respecter 4 m de largeur. Pour les autres types de zonage, il faut respecter 10 m et 15 m de largeur lorsque la pente est inférieure à 30% ou supérieure à 30% respectivement.

Au préalable, le MNT satellitaire a suivi un reconditionnement au niveau des voies d'écoulement à l'intérieur des parcelles agricoles. Ce reconditionnement du MNT a pour finalité d'imposer les

voies d'écoulement. Cette information a été extraite à l'aide de la numérisation sur écran en utilisant l'image printanière où les champs agricoles ne sont pas couverts par la végétation et les voies d'écoulement étant facilement identifiables. Ceci était nécessaire afin d'améliorer l'extraction de variables sur l'écoulement des eaux et de mieux interpréter la configuration hydrologique qui existe entre la parcelle et ses bandes riveraines. Ensuite, l'IQBR (Éq. 2.2) a été calculé de façon automatique pour chaque bande riveraine du bassin versant en utilisant la carte de végétation en format vectoriel et le MNT satellitaire à 0,5 m de résolution spatiale.

Afin d'évaluer l'efficacité des bandes riveraines en milieu agricole, l'IQBR a été combiné à un indicateur de la qualité du drainage (QD). L'analyse a été faite dans les sections de cours d'eau d'une longueur définie par les côtés des parcelles en contact avec les bandes riveraines (Fig. 2.7). Cet indice vise à catégoriser les bandes riveraines en fonction de leur capacité à intercepter les eaux de ruissellement. Les variables utilisées pour le calcul sont : (i) la superficie drainée cumulée par les exutoires extrêmes et (ii) la superficie totale de la parcelle en étude. L'indice de la qualité du drainage, dont la valeur varie de 0 (bonne) à 1 (très faible), est calculé comme suit :

$$QD = \sum (drainage_{P75}) \, / \, superficie\ parcelle \qquad\qquad (2.4)$$

où $\sum(drainage_{P75})$ représente le cumul des superficies drainées des exutoires ayant un percentile plus grand que 75, et *superficie parcelle* représente la superficie totale de la parcelle agricole qui est en contact avec la bande riveraine en étude.

Dans la Figure 2.7 on peut constater que les deux bandes riveraines reçoivent potentiellement différentes quantités d'eau de ruissellement. Donc, celle qui contient des exutoires extrêmes a une qualité du drainage faible (en couleur orange). Par contre, la bande riveraine en couleur verte n'a aucun exutoire extrême, ce qui se traduit dans une bonne qualité du drainage.
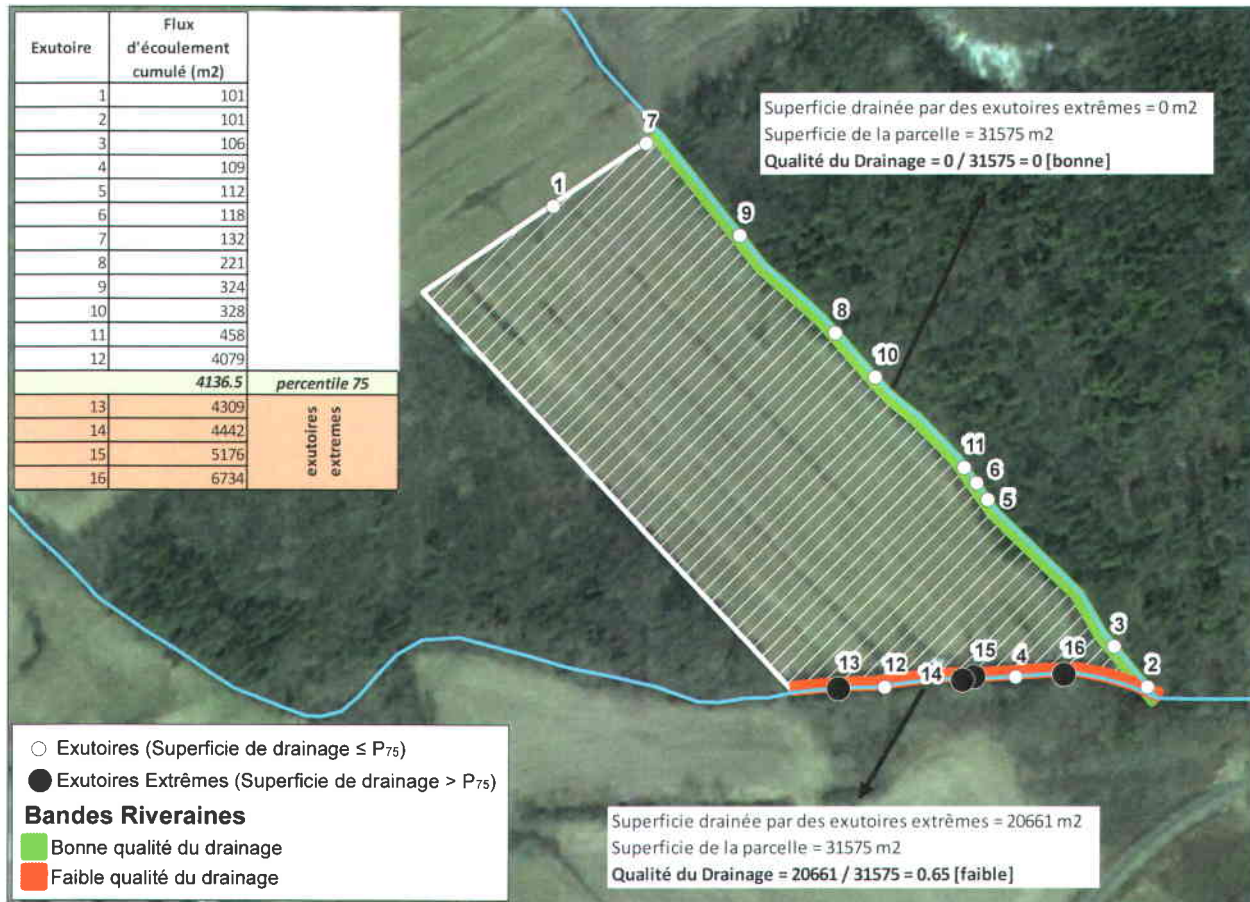
Figure 2.7 : Configuration du drainage d'une parcelle agricole.

Une fois l'IQBR et la QD calculés, ceux-ci ont été catégorisés en quatre classes : très faible, faible, moyen, et bon (Tableau 2.2).

Tableau 2.2 : Catégorisation de l'indice de qualité écologique (IQBR) et de la qualité du drainage (QD) des bandes riveraines.

Catégorie	IQBR	QD
Très faible	< 40	> 0,75
Faible	40 – 60	0,50 – 0,75
Moyenne	60 – 80	0,25 – 0,50
Bonne	> 80	< 0,25

Enfin, à partir de l'analyse combinée de l'indice de qualité et la qualité du drainage de la bande riveraine, l'indice d'efficacité a été calculé comme suit :

Indice d'efficacité = min (IQBR, QD)   (2.5)

3   RÉSULTATS

3.1   Qualité du modèle numérique du terrain satellitaire

Malgré l'existence d'une erreur systématique de 0,78 m qui se traduit par une surestimation de l'élévation dans le MNT satellitaire, ce dernier représente bien l'élévation dans la zone à l'étude. Ce biais est communément causé par l'opérateur au moment du calage spatial de l'image satellitaire stéréoscopique avec des points de control GPS à très haute précision. Étant donné sa nature d'erreur systématique, elle est corrigeable. Après correction, et en se basant sur les critères d'évaluation altimétrique communément utilisés dans les rapports de précision de produits géospatiaux, il a été constaté que globalement le modèle satellitaire représente assez fidèlement l'élévation sur les parcelles agricoles. Ainsi, l'erreur quadratique moyenne est de 0,23 m, l'erreur verticale LE90 est de 0,36 m, et la précision verticale (Az) est de 0,45 m. La précision de ce MNT satellitaire pourrait être comparée à celle obtenue par un jeu de données LiDAR avec un espacement nominal entre points de trois mètres ou moins, et une densité minimale de quatre points par mètre carré.

Après vérification de la précision verticale et la correction du biais du MNT satellitaire, il a été testé dans sa capacité à représenter le microrelief. Ceci a été réalisé en analysant trois variables : la pente, les dépressions du terrain et les voies d'écoulement. Pour ce faire, un MNT, crée à partir du jeu de données GPS-RTK, a été utilisé comme modèle de référence. Les pentes longitudinales (pente dans la direction principale de l'écoulement des eaux) affichent des variations de moins de 1% par rapport au modèle de référence. Les pentes moyennes et maximales présentent des variations de 27% et 22% respectivement. Par rapport aux dépressions topographiques, le modèle satellitaire a eu de la difficulté à bien les définir, tant en quantité qui en superficie, avec des variations de plus de 70%. Quant aux voies d'écoulement, les longueurs moyennes, maximales et totales ont présenté des variations de 47%, 57% et 18% respectivement. Et pour finaliser cette analyse, des variations de 76% et 90% ont été obtenues pour le nombre d'exutoires et la superficie drainée cumulée respectivement. Il faut noter que

pour les zones agricoles ayant une pente longitudinale supérieure à 5%, les variables pente et voies d'écoulement ont montré de variations mineures, ce qui pourrait permettre leur utilisation dans la modélisation environnementale (voir Section 5).

3.2 Qualité et efficacité de la bande riveraine

La classification orientée-objet a bien performé dans l'extraction d'information sur l'utilisation du sol. Les catégories *végétation arborescente*, *cultures*, *sol nu* et *infrastructure* ont été les plus précises, avec des coefficients de concordance élevés (K>0,92), tandis que les catégories *végétation arbustive*, *végétation herbacée naturelle* et *friche/fourrage/pâturage/pelouse* ont présenté les coefficients de concordance les plus faibles (0,39<K<0,67). Globalement, la carte de végétation a un indice de concordance K de 0,82.

À partir de la carte de végétation et le modèle numérique du terrain satellitaire, l'indice de qualité de la bande riveraine (IQBR) a été calculé. Ainsi, avec un IQBR global moyen de 69, en suivant la classification de l'IQBR faite par le MDDEFP, le bassin versant appartient à la catégorie de qualité écologique *moyenne*. Pour évaluer la performance de ces analyses, une comparaison a été faite en zones agricoles entre les données relevées sur le terrain manuellement (IQBR=55) et les résultats obtenues avec la classification orientée-objet (IQBR=56). Les résultats sont prometteurs, car la différence est minimale entre les IQBR moyen des deux sources de données. De plus, l'IQBR moyen des zones non-agricoles du bassin versant a une valeur de 80, c'est-à-dire qu'elles ont une bonne qualité écologique.

En termes d'efficacité, les bandes riveraines ont de la difficulté à remplir leur fonction écologique dans les zones agricoles. Il est évident que lorsqu'on ajoute à l'IQBR la *Qualité du drainage* (QD), ce dernier paramètre aide notablement à faire une meilleure discrimination des bandes riveraines. Pour citer un exemple, dans les bandes riveraines avec un Bon IQBR, il est facile à visualiser que la plupart (71,9%) de ces bandes riveraines demeurent dans la catégorie *Bonne efficacité*, c'est-à-dire qu'elles sont couvertes d'une végétation naturelle et la configuration de drainage a le potentiel de filtrer et retenir les sédiments qui proviennent des eaux du ruissellement agricole. Par contre, 21,2% de ces bandes riveraines avec un Bon IQBR appartiennent à la catégorie *Moyenne efficacité*, 6,5% à la catégorie *Faible efficacité* et *0,5%* à la catégorie *Très faible efficacité*. Ce recul dans les catégories est causé évidement par la qualité du drainage de la bande riveraine. Le Tableau 3.1 illustre la répartition des catégories de l'IQBR et de l'efficacité des bandes riveraines :

Tableau 3.1 : Répartition des catégories de l'IQBR et de l'efficacité des bandes riveraines

Catégorie	Longueur (km)	%
Bon IQBR	31,78	
*Bonne efficacité**	*22,84*	*71,9%*
Moyenne	*6,74*	*21,2%*
Faible	*2,05*	*6,5%*
Très faible	*0,15*	*0,5%*
Moyen IQBR	17,40	
Moyenne	*14,88*	*85,5%*
Faible	*2,31*	*13,3%*
Très faible	*0,21*	*1,2%*
Faible IQBR	26,50	
Faible	*26,35*	*99,4%*
Très faible	*0,15*	*0,6%*
Très faible IQBR	34,39	
Très faible	*34,39*	*100%*
TOTAL	110,08	

* Catégories d'efficacité de la bande riveraine en italiques.

4   CONCLUSIONS

Le modèle numérique de terrain (MNT) du bassin versant La Chevrotière dérivé du satellite WorldView-2 a été évalué à la fois dans sa précision verticale et dans sa capacité à représenter le microrelief. Pour ce faire, un ensemble de points GPS-RTK, à très haute précision et à très haute densité, a été utilisé pour analyser la performance du MNT satellitaire. Il en résulte que le MNT extrait du satellite WorldView-2 a une précision verticale de 0,45 m. Ceci est conforme aux spécifications techniques du fournisseur du MNT satellitaire, dont la précision verticale minimale garantie est de 1,0 m. Par conséquent, le MNT dérivé de l'imagerie satellitaire à très haute résolution spatiale constituerait ainsi une source de données d'élévation avec une précision verticale acceptable. Ces données s'avèrent également abordables étant donné que cette précision verticale est comparable à celle qu'on pourrait obtenir à partir des données LiDAR à faible densité (4 points/m^2).

Par rapport à sa capacité à représenter le microrelief, il s'avère que le MNT satellitaire a de la difficulté à bien représenter la variabilité de la microtopographie en comparaison à celui produit à partir des points GPS-RTK. En effet, les variables topographiques analysées (pente, dépressions, voies d'écoulement), dérivées du MNT satellitaire sont moins précises que celles estimées à partir des points GPS-RTK. Ainsi, le MNT satellitaire semble incapable de saisir les

variations topographiques à l'échelle spatiale plus fine que sa résolution spatiale (1 m x 1 m). Afin de pallier à ce problème, il est possible d'exploiter l'information spectrale contenue dans la paire d'images stéréoscopiques pour corriger localement le MNT satellitaire et améliorer ainsi sa capacité à représenter le microrelief à l'échelle de la parcelle. Par exemple, l'information spectrale dans l'infrarouge permettrait de détecter et de délimiter les dépressions de terrain au printemps étant donné qu'elles sont généralement plus humides que le reste du terrain. L'élévation de ces dépressions pourrait être corrigée en conséquence. Dans le présent projet, le tracé des voies d'écoulement obtenu par numérisation à l'écran sur les images à très haute résolution spatiale a été utilisé pour améliorer la représentation du microrelief.

La qualité et l'efficacité des bandes riveraines du bassin versant La Chevrotière ont été par la suite évaluées à partir de l'information multispectrale et altimétrique provenant du satellite WorldView-2. Ainsi, l'évaluation de l'indice de qualité de la bande riveraine (IQBR) s'est basée sur le protocole technique développé par le MDDEFP. Toutefois, la méthodologie proposée a été modifiée en remplaçant les observations sur le terrain et la photographie aérienne (procédés laborieux et coûteux) par une approche automatique basée sur la classification orientée-objet et l'analyse spatiale de l'information satellitaire à très haute résolution spatiale. L'avantage de cette approche méthodologique réside dans sa rapidité d'exécution et de ses coûts associés plus faibles que la méthode conventionnelle. En effet, évaluer la qualité et l'efficacité des ~320 km des bandes riveraines du bassin versant à l'étude occuperait à temps plein un opérateur pendant trois à quatre semaines. En revanche, ceci lui prendrait facilement trois fois plus temps pour réaliser le même travail à l'aide la méthode conventionnelle.

Pour ce qui est de la qualité de la carte de végétation obtenue à partir de la classification orientée-objet, la concordance trouvée entre les données relevées sur le terrain est celle obtenue à partir de la méthodologie proposée permet de confirmer la pertinence de l'utilisation de ce type d'images satellitaires pour évaluer la qualité écologique des bandes riveraines. Il a été démontré que la plupart de problèmes environnementaux en lien avec les bandes riveraines, se trouvent dans les zones agricoles du bassin versant. À ce titre, l'IQBR passe d'une valeur de 69 (qualité écologique moyenne) pour tout le bassin versant à 56 (qualité écologique faible) en zones agricoles. Par ailleurs, l'ajout de l'information sur la qualité du drainage à l'IQBR a permis de mieux discriminer les bandes riveraines inefficaces du point de vue écologique. Cette incorporation de la qualité du drainage a donné origine à l'indice d'efficacité de la bande riveraine. Ceci permettra aux organismes de bassin versant d'optimiser leurs efforts financiers et

leurs ressources humaines déployés et de les concentrer sur les bandes riveraines plus problématiques.

ARTICLES SCIENTIFIQUES

5 HYDROLOGICAL ASSESSMENT OF A DEM DERIVED FROM WORLDVIEW-2 REMOTE SENSING DATA

Julio Novoa*[1], Karem Chokmani[1], Rody Nigel[1], & Philippe Dufour[2]

[1]*Institut national de la recherche scientifique (INRS), Centre Eau-Terre-Environnement (ETE), 490, de la Couronne, Québec (QC) G1K 9A9*
[2]*CAPSA, 111-1, route des Pionniers, St-Raymond (QC) G3L 2A8*

Abstract

A digital elevation model (DEM) derived from a stereoscopic pair of WorldView-2 (WV-2) images was assessed against ground-truth GPS point data sets. Two assessment methods were used: (i) vertical accuracy assessment and (ii) hydrological assessment of surface runoff variables. Three agricultural fields, with different topographic slopes, were selected to perform a vertical accuracy assessment, followed by a comparative assessment of a set of hydrological variables. Results show a global vertical accuracy of 0.45 m, confirming the potential of WV-2 stereoscopic images to extract elevation information at high spatial resolution. Concerning field-scale micro-topographic features, the WV-2 DEM performed better on the field with rolling slopes (5–10%), extracting variables such as the total length and drainage area of flow paths with relative errors lower than 20%. However, some limitations were detected in the extraction of variables such as terrain slope, drainage points of flow paths, and terrain depressions in areas of flatter areas (<5%).

5.1 Introduction

Gridded digital elevation models (DEM) are used in many disciplines to represent topographic characteristics required in landscape, hydrological, and erosion modelling (Li *et al.*, 2005, Longley, 2005). The uses of DEMs in hydrological analysis include, among others, (i) automatic extraction of terrain properties and drainage networks, (ii) determination of flow direction and accumulation, (iii) delineation of catchment areas, and (iv) extraction of watercourses, among others (Nigel *et al.*, 2010a, Wechsler, 2007).

Several studies have been conducted at the basin scale to analyse the capabilities and limitations of DEMs in hydrological modelling (e.g. Callow *et al.*, 2007, Hage *et al.*, 2012, Hosseinzadeh, 2011, Rezak *et al.*, 2012). However, at larger scales there is a lack of knowledge to support operational and practical uses of DEMs (Lyon *et al.*, 2003), particularly for cropland, where it is anticipated that high-resolution data can provide farmers with accurate topographic information to develop better, more productive, environmentally conscious practices to increase yield while decreasing environmental impacts (Ge *et al.*, 2011, Velde *et al.*, 2010).

Lowland watersheds—generally characterized by fertile soils, water availability, and high accessibility—are commonly exploited for urbanization or agricultural practices. This gives rise to environmental problems such as soil loss and water pollution (e.g., high nutrient inputs,

modifications of water flow paths, etc.). In hydrological modelling, it is essential to evaluate topographic representations of watersheds using DEMs (Velde *et al.*, 2010). Among the DEM-extracted topographic variables most used in hydrological modelling are slope, flow path, drainage area, watershed area, and combined variables such as the topographic index (Wu *et al.*, 2008). Several studies (Chaubey *et al.*, 2005, Wolock *et al.*, 1994, Zhang *et al.*, 1994) have confirmed that at lower spatial resolution, slopes decreases and drainage area increases, reducing the topographic index values. The latter is a key factor in many distributed hydrological models because it is used for estimating the spatial distribution of groundwater levels, surface saturation, and runoff discharge (Mukherjee *et al.*, 2013). Accordingly, increasing coarseness of the DEM tends to decrease the mean depth of water table, and to increase daily and total flow. Moreover, surface saturation and surface runoff peak discharges increased when the DEM spatial resolution decreased. Using TOPMODEL, a topographic-based tool to simulate hydrologic flux in a watershed, flow length and watershed area did not show a systematic pattern as a function of DEM spatial resolution, fact confirmed by Charrier *et al.* (2012) when analysing LiDAR-derived DEMs. Nevertheless, Chaubey *et al.* (2005) detected a pattern when evaluating outcomes from the Soil and Water Assessment Tool (SWAT), where watershed and sub-watershed delineation at coarser spatial resolutions presented smaller areas compared to ground truth. The impact of flow lengths in hydrological modelling has also been evaluated and results showed there might be a time lag between precipitation and flow peak discharge, altering the predicted hydrographs (Wu *et al.*, 2008). Indeed, water streams length tend to gradually decrease with a coarser DEM spatial resolution, but in the prediction of floodplain boundaries, flooded surface tends to increase (Charrier *et al.*, 2012). These parameters are extremely important at field scale because flow paths determine the hydrologic connectivity of saturated areas in croplands, thus, a wrong flow path extraction and micro-watershed delineation could lead to erroneous estimations (Shore *et al.*, 2013).

High-precision DEMs are required in hydrologic modelling in order to produce unbiased predictions and outcomes (Lin-Lin *et al.*, 2010, Vaze *et al.*, 2010). Accurate elevation information is an important component of hydrologic modelling at high spatial resolution. DEM-extracted variables such as water flow direction and accumulation, micro-basins, flow paths, drainage points, depression zones, and drainage area need to be derived from highly accurate elevation models (preferably at high resolution too) to ensure good quality outcomes (Erskine *et al.*, 2007).

Currently, a variety of remote sensing techniques are used to generate elevation models. These techniques, most of which have been developed and improved over the last thirty years (Toutin

et al., 2002), range from standard and GPS topography, aero- and space-photogrammetry, and radar interferometry to airborne LiDAR. Some drawbacks of these technologies are cost, processing time, and lack of diversified spectral information (with the notable exception of space photogrammetry) (Hobi *et al.*, 2012).

Very high spatial resolution (VHSR) stereoscopic satellite images, defined as imagery with pixels sizes of 1 metre or less, have been commercially available since the launch of the IKONOS satellite in 1999. VHSR satellite stereoscopic images are being used as a viable and fast alternative for producing elevation models (Jacobsen, 2004). The WorldView-2 satellite, launched in October 2009, is equipped with panchromatic and multispectral sensors, and is capable of capturing stereoscopic images. These pairs of images can be used in automatic elevation extraction processes to generate DEMs covering the areas of the images. In addition, the satellite's revisit time of 1–4 days makes it an important source of data for monitoring spatial phenomena over time. WorldView-2 is the first satellite with one panchromatic band and eight multispectral bands at 0.5 m and 2 m spatial resolution, respectively. The panchromatic sensor can capture pairs of stereoscopic images to be used to generate 1-m pixel size DEMs. Previously, such high-resolution stereo-based DEMs were only achievable with aerial photogrammetry and land surveying (Büyüksalih *et al.*, 2012).

The aim of this research is to evaluate, at the agricultural field scale, the capabilities and limitations of a WorldView-2 digital elevation model (WV-2 DEM) for representing elevation and extracting hydrologic variables commonly used in environmental modelling. The WV-2 DEM will be evaluated against high-density and high-precision field-captured GPS point data sets based on an assessment of (i) vertical accuracy and (ii) extracted hydrological variables describing spatial surface runoff.

5.2 Methods

5.2.1 Study Area

The La Chevrotière River basin is located in the Portneuf Municipality, part of the Capitale-Nationale Administrative Region, in the province of Quebec, Canada (Fig. 5.1). The basin lies on the north shore of the St. Lawrence River and has an area of 108 km^2. It is located in a low-lying region that is mainly agricultural, characterized by pasture, forest patches, and small urban settlements. The combined population of Saint-Marc-des-Carrières and Saint-Gilbert, the two

main urban centres, is around 3100 inhabitants. The La Chevrotière River is the convergence of two main branches and several small tributaries. It covers a distance of 29 km in a flat-to-undulating landscape before reaching the St. Lawrence. The highest point in the river basin has an altitude of 150 m above sea level. The mean slope of the basin is around 5%, but in riverine zones, slopes can be greater than 8% (Capsa, 2011).
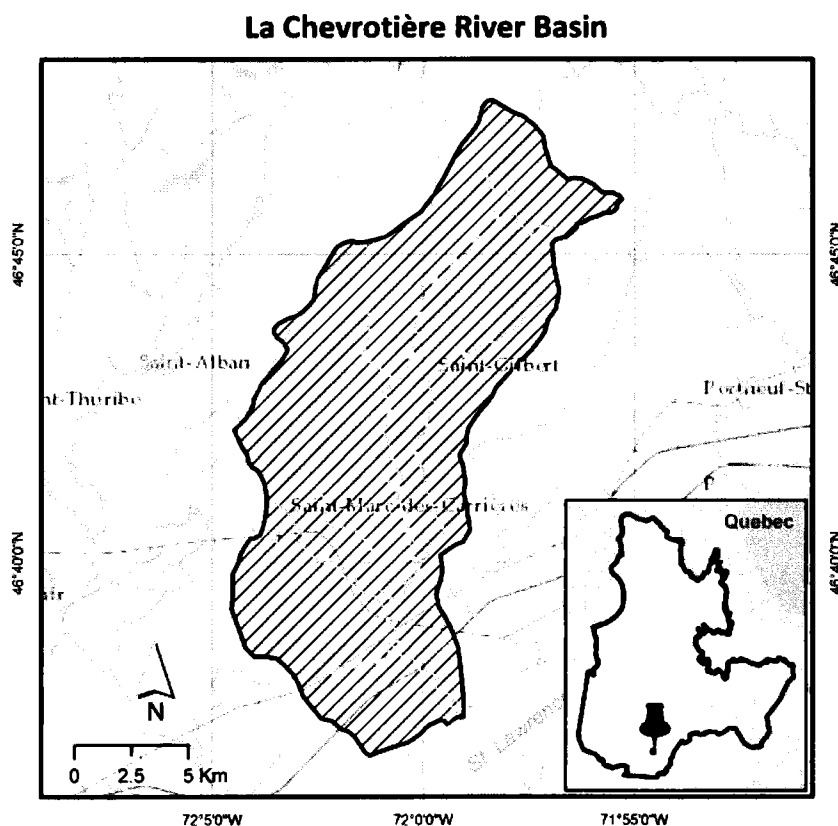
Figure 5.1: The study area, the La Chevrotière River basin (107 km^2), located on the north shore of the St. Lawrence River in the province of Quebec, Canada.

Like most river basins in agricultural regions, the La Chevrotière basin faces a variety of environmental pressures, including nonpoint source pollution, and soil loss (Capsa, 2011). Many of these environmental problems are being addressed from a landscape perspective, creating an operational gap between land managers and planners—who work at regional scales—and the occupants of the basin—who work at local scales and who typically lack technical information to understand and participate in the territorial planning process of their watershed. Tools to foresee potential problems at smaller analysis scales (e.g., agricultural fields) would

give landscape planners a way to evaluate the potential hydrological problems faced locally (on fields) by farmers. Such tools would also provide farmers and other watershed inhabitants information that could prevent environmental problems and improve their income through better practices. Provision and use of such tools would represent a viable, empowering management practice that could improve water quality and reduce environmental impacts (Lyon *et al.*, 2003, Velde *et al.*, 2010).

5.2.2 Data Description

This research is based on two data sets: (a) high-precision and high-density GPS point data sets from field surveys (hereinafter referred to in tables and figures as *GPS*) and (b) a 1-m gridded digital elevation model with a vertical accuracy of 1 m extracted from a WorldView-2 stereoscopic pair (hereinafter referred to in tables and figures as *WV-2*).

5.2.2.1 Ground-Truth GPS survey

During summer 2011, we carried out ground-truth GPS surveys in three agricultural fields with different topographic characteristics. Field 1 has a nearly level longitudinal slope of 0.3% (the longitudinal slope covers the length of the field and is indicated by the arrow in the field in Fig. 5.2). The elevation range of the field is 2.3 m, and its maximum slope is 25%. Field 2 has a gentle longitudinal slope (1.0%), maximum slopes of ~27%, and an elevation range of 4.6 m. Field 3 has a nearly rolling longitudinal slope (5.2%) and an elevation range of 17.4 m, with a maximum slope of 63%.
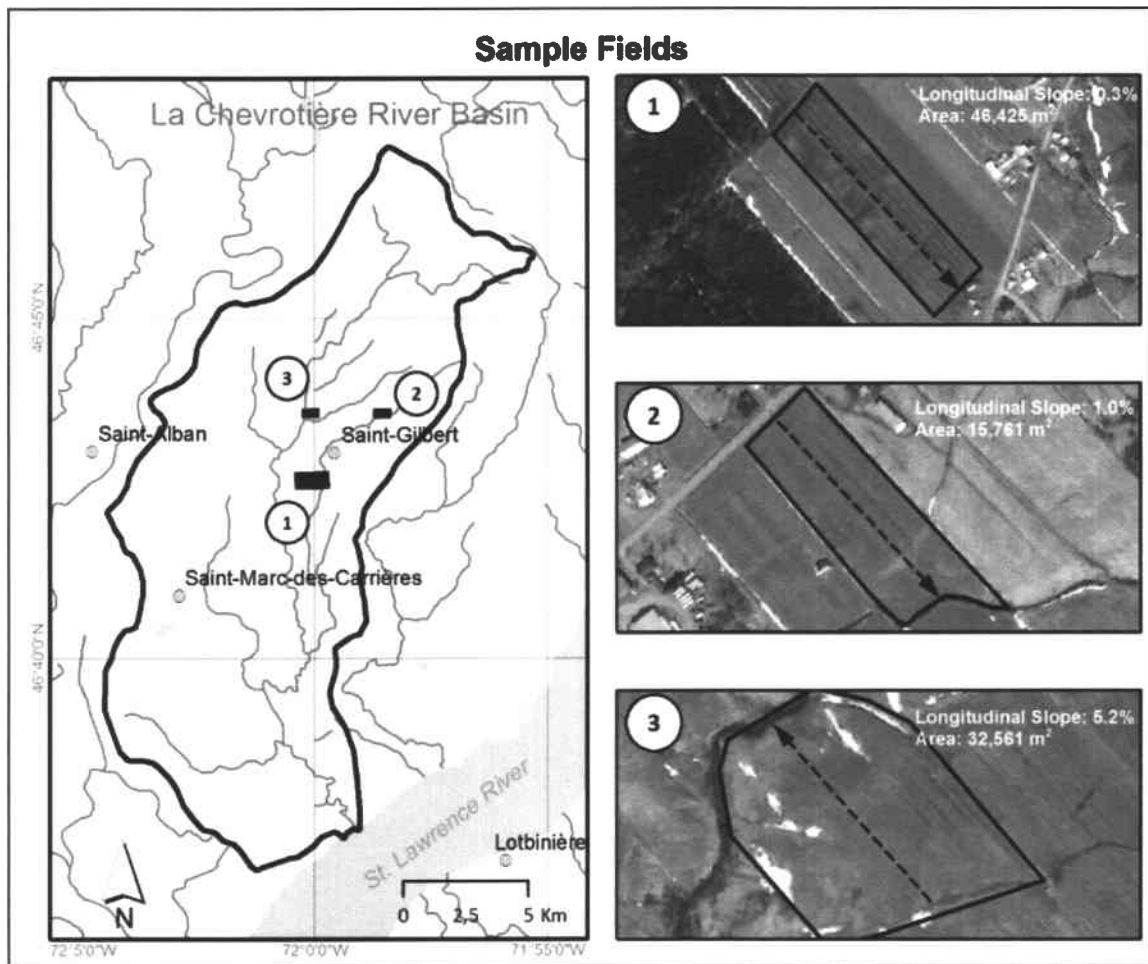
Figure 5.2: The three agricultural fields used for ground-truth GPS-RTK survey. The arrow in each field represents the longitudinal slope used for describing the topography of the field.

For this project, we mounted a GPS receiver on an all-terrain vehicle and, using a differential real-time kinematic (RTK) method, collected 131,519 xyz coordinates from a well-distributed grid of points, evenly spaced on the ground approximately every meter. The resulting data set had an average density of 1.5 GPS points per square meter and a vertical accuracy of 10 cm (Table 5.1). As discussed in Hohle *et al.* (2009), the quantity and accuracy of the control points surveyed must be at least three times as great as those of the evaluated DEM. In the present work, this requirement was surpassed to ensure a correct comparative statistical analysis.

Table 5.1 : Ground-truth data set statistics.

Elevation	Field		
(m)	1	2	3
Minimum	66.77	83.89	58.66
Maximum	69.05	88.44	76.12
Range	2.28	4.56	17.44
Mean	68.08	87.29	71.54
Median	68.11	87.85	73.72
Standard Deviation	0.35	1.15	4.95
Longitudinal Slope (%)	0.3	1.0	5.2
GPS points collected	40 603	23 603	67 313

5.2.2.2 Satellite DEM

The satellite stereoscopic pair of images was taken by the WorldView-2 VHSR satellite on 14 April 2012 (15:58 and 15:59 GMT). The images were in UTM projection and WGS84 datum. In order to geo-rectify the images, we provided the image supplier (in the present case, Effigis Inc., http://effigis.com) with five ground control points. The ground control points were selected from well-distributed and easily recognizable image features, such as utility poles and the intersections of paved streets. The image supplier then took the images and control points and generated an ortho- and geo-rectified Digital Elevation Model (DEM) using the BAE Systems NGATE module (Devenecia *et al.*, 2007). That module applies image correlation algorithms to automatically extract elevation. During the process, image features such as roads, tracks, rivers, railways, freeways, etc., are additionally extracted using image interpretation and integrated into the DEM. The output DEM was in the local coordinates of MTM7 projection and NAD83 datum. Supplier's quality standard in horizontal and vertical accuracy were both 1 m.

The two data sets (GPS points and WorldView-2 DEM), were then compared using two complementary assessment techniques. The first analysed the ability of the NGATE module to extract accurate elevation values in the form of a gridded model, and the second performed a comparative evaluation of geomorphological and drainage variables extracted from the satellite DEM and the GPS-based DEM over the three sample fields.

The three fields used in the GPS survey were not tilled and bare of plant life, with topographic features clearly visible, during the field survey (summer 2011) and subsequent satellite image capture (spring 2012). However, there are small concave areas on the satellite image—mainly in Field 3—where terrain characteristics were not extracted properly (during DEM generation)

34

because of the presence of snow during image acquisition (the discussion section will include some comments on this issue).

5.2.3 Vertical Accuracy Assessment

For the elevation accuracy assessment, we used widely applied metrics such as Mean Absolute Error (MAE) and Root Mean Square Error (RMSE) (Eckert *et al.*, 2005). Additionally, and to make this study comparable to other research and to commercially available digital elevation model accuracy reports, we also calculated metrics such as 90th percentile linear error (LE90) and vertical accuracy at 95% confidence level (Asprs, 2007). To accurately calculate absolute vertical accuracy, each sample field was analysed individually. For this, at the location of each ground-truth GPS point, the corresponding elevation provided by the satellite DEM was extracted. We used this approach to avoid errors introduced by interpolation algorithms.

5.2.4 Hydrological Assessment

It is well known that physically-based hydrological models make use of gridded digital elevation models to extract basic topographic variables in order to simulate several phenomena in a watershed. Those variables are then used to simulate or predict hydrological processes and outcomes such as surface runoff, or they are used as input datasets for further analyses, for example, in sediment, nutrient, pollutant transport, erosion and natural hazards modelling, or assessing biological diversity (Moore *et al.*, 1991).

The hydrological assessment method used in this work relies on geomorphological and drainage variables derived from a grid DEM. Therefore, for this assessment, the GPS points were interpolated to generate a DEM for each field. The DEMs were interpolated at 1-m resolution using the Inverse Distance Weighted (IDW) algorithm. This interpolation algorithm performs well when the density and precision of the source elevation data are high (Aguilar *et al.*, 2010, Chaplot *et al.*, 2006, Guo *et al.*, 2010, Lin-Lin *et al.*, 2010). Our GPS data set met both of these conditions, with an average point density of 1.5 points per square meter and a vertical accuracy of 10 cm.

One quarter of the GPS points were randomly selected for validation purposes (i.e., not used in the interpolation process). As expected, small interpolation errors (0.03 m) were found in the three fields. However, such errors are more sensitive to the DEM's sources than to interpolation algorithms and uncertainties (Erskine *et al.*, 2007, Li *et al.*, 2012). We concluded that the IDW

algorithm was an appropriate choice, offering a good balance between accuracy and computing speed.

The variables retained for assessment were: (1) terrain depressions, (2) terrain slopes, (3) and flow paths. These variables, and their quality indicators, were chosen to ensure an easily reproducible hydrologic quality assessment using available software and the simplest variables (Table 5.2). In the present case, the quality indicators were extracted using the software ArcGIS® (http://esri.com) and its ArcHydro® module, which is extensively used in hydrological analyses as it is effective at extracting hydrological parameters for further modelling (Maidment, 2003, Nigel *et al.*, 2010b, Zhang *et al.*, 2010).

Table 5.2 : Geomorphological and drainage variables.

Variable	Quality Indicators	Output Information
Terrain Depressions	Depressions' Total Area Depressions' Non-Overlapping Area	Vector Polygons
Slope	Longitudinal Slope Mean Slope Maximum Slope	Raster Layers
Flow Paths	Flow Paths' Mean Length Flow Paths' Maximum Length Flow Paths' Total Length Drainage Outlets Drainage Area	Vector Points and Polylines

Pits or depressions are low points completely surrounded by higher elevation points. These features pose the main difficulty in determining surface drainage because the depressions must be filled before flow can continue downstream (Jenson *et al.*, 1988b). Thus, a DEM that can correctly identify and represent depressions or pits can provide important information at the agricultural field scale; such information is directly related to nutrient control and crop yields and has wide potential use in precision agriculture (Lyon *et al.*, 2003). DEM post-processing for hydrologic and erosion modelling produces a "filled" DEM from which pits are removed. To identify the location of depressions, we extracted terrain depression polygons by subtracting the original DEM from this "filled" version. In order to evaluate the performance of the model using this technique, two quality indicators were used: total area of depressions and non-overlapping areas of depressions. The first expresses the quantity of land surface detected as a depression, while the second expresses the spatial coincidence of these depressions over the surface.

After terrain depressions, terrain slopes were extracted. In a gridded DEM, slope is a local function, and it represents the maximum rate of elevation change of a plane formed by a 3x3-cell

neighbourhood around the centre pixel (Eq. 5.1). The slope value of this plane was calculated using the average maximum technique (Burrough, 1986) over the distance between the target cell and its surrounding eight pixels, and it is expressed in decimal degrees as

$$\text{slope} = \arctan \left[\sqrt{ \left((dz/dx)^2 + (dz/dy)^2 \right) } \right] \tag{5.1}$$

where dz/dx is the rate of elevation change in the east–west direction and dz/dy is the rate of elevation change in the north–south direction of the plane. To evaluate the performance of this variable, three quality indicators were used: the longitudinal slope (Fig. 2), the mean slope, and the maximum slope.

Finally, flow paths were extracted, and to evaluate their performance five quality indicators were calculated: mean length, maximum length, total length, drainage outlets, and drainage area. The first three indicators are directly derived from the geometric properties of flow paths, while the other two—drainage outlets and drainage area—are extracted indirectly. Drainage outlets give precise information of the position at which water flows out of a catchment area, while drainage area corresponds to the total area drained towards the drainage point; the latter is commonly used as a proxy of potential runoff volume. To calculate these five indicators, intermediate data sets such as flow direction and flow accumulation were extracted. The ArcHydro software uses a pre-filling algorithm to calculate flow direction (Jenson *et al.*, 1988b), which ensures a continuous water flow and enables further hydrological modelling. The flow direction algorithm used by the software, called D8, uses the direction of the steepest descent from the central pixel of a 3x3 moving window to one of its eight neighbours to determine the direction of water flow in every cell of the elevation model. Subsequently, flow paths were extracted using an accumulation threshold of 100 cells (i.e., 100 m^2), which was selected after several tests were performed to determine the number of cells needed to ensure good, continuous representation of the surface runoff flow paths. Due to the importance of knowing the position and amount of water flow towards natural water streams or artificial pathways, an individual analysis was made for each side of the sample fields (i.e., northeast, northwest, etc.).

Once the geomorphological and drainage variables were calculated, and in order to ensure easy comparability between the variables and across the three sample fields, we used the relative error (e), expressed in percentage terms (Eq. 5.2), as a relative measure of change, as follows:

$$e = \left[(value - value_{ref}) / value_{ref} \right] \times 100 \tag{5.2}$$

where *value* corresponds to the measured value from the satellite DEM and *value*$_{ref}$ is the ground-truth value extracted from the GPS-derived elevation model. This metric is frequently used when absolute values are expressed in different units or different magnitude scales. It must be noted that neither of the two elevation models, GPS and WV-2, were post-treated with drainage enforcement procedures in order to impose linear or polygonal entities, particularly to enforce flow direction.

5.3 **Results and Discussion**

5.3.1 **Vertical Accuracy**

First, we analysed the elevation residuals using the GPS points collected in every field (Table 5.1). This enabled us to identify the presence of a systematic elevation error (bias), with a global mean value of 0.78 m, revealing a trend of the satellite DEM to systematically overestimate the elevation in bare, flat terrain (Fig. 5.3). There are two error categories in elevation models: random and systematic. The latter category originates mostly in the production chain, which is composed of processes that make use of image matching, elevation extraction, and gridding algorithms (Wise, 2000). Similar elevation biases have been found in other DEMs derived from imagery from WorldView-2 and other satellites (Büyüksalih *et al.*, 2012, Li *et al.*, 2012, Reinartz *et al.*, 2010). As these examples show, systematic errors are commonly present in satellite-derived elevation products. It is preferable that such errors be detected and eliminated before further processing, particularly in studies requiring absolute DEM values or operating at very high spatial resolution.
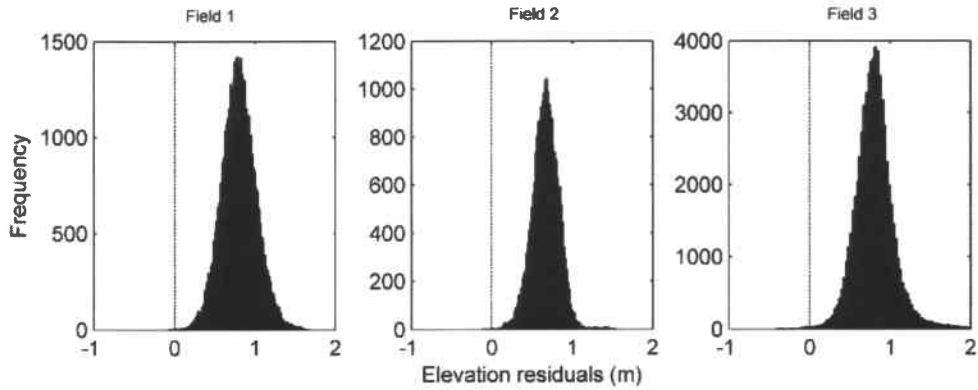
Figure 5.3: Histograms of elevation residuals of the sample fields.

Table 5.3 shows the accuracy metrics calculated using the biased elevation residuals. We found a global Root Mean Square Error (RMSE) of 0.81 m, a Vertical Accuracy of 1.60 m, a Mean Absolute Error of 0.78 m, a global Maximum Absolute Error of 2.36 m, and a Vertical Linear Error (LE90) of 1.05 m.

Table 5.3 : Biased vertical accuracy metrics (m) of the WorldView-2 DEM.

Field	Bias	RMSE	Vertical Accuracy	MAE	Maximum Absolute Error	LE90
1	0.80	0.83	1.63	0.80	1.67	1.08
2	0.67	0.69	1.34	0.67	1.53	0.87
3	0.81	0.84	1.66	0.81	2.36	1.08
Global	0.78	0.81	1.60	0.78	2.36	1.05

Before further analysis, we removed the 0.78-m bias in order to obtain adjusted error metrics of the elevation model (Vaaja *et al.*, 2011). Once the bias was removed (Table 5.4), we found a global Root Mean Square Error (RMSE) of 0.23 m, a Vertical Accuracy of 0.45 m, a Mean Absolute Error of 0.17 m, a global Maximum Absolute Error of 1.55 m, and a Vertical Linear Error (LE90) at the 90th percentile of 0.36 m.

Table 5.4 : Vertical accuracy metrics (m) of the WorldView-2 DEM.

Field	RMSE	Vertical Accuracy	MAE	Maximum Absolute Error	LE90
1	0.22	0.42	0.17	0.88	0.36
2	0.17	0.33	0.13	0.87	0.56
3	0.25	0.49	0.18	1.55	0.38
Global	0.23	0.45	0.17	1.55	0.36

In brief, the WV-2 DEM achieved a vertical accuracy of 0.45 m, consistent with the quality standards of the supplier. The WV-2 DEM vertical errors obtained in this work are similar to those found in other studies using WorldView-2 images, particularly those focused on analysing DEM performance on bare land (Hobi *et al.*, 2012, Mitchel *et al.*, 2010). This confirms both the capabilities of the satellite-derived elevation model and the correctness of the present methodology and data used.

In addition to our analysis of vertical accuracy metrics, we made a visual comparison of transversal elevation profiles of the sample fields to evaluate the capabilities of the satellite DEM to detect micro-topographic features (Fig. 5.4). In the GPS-based DEM (solid line), we can clearly observe the micro-relief defined by the longitudinal water flow paths (valleys) and the cultivable areas (crests). Conversely, the WorldView-2 DEM (dotted line) shows mostly a smoothing effect in elevation, producing a flattening in all profiles. The NGATE elevation extraction algorithm, which is a hybrid algorithm that uses a variably sized search window to apply edge and area matching correlation algorithms to every pixel of the image (Devenecia *et al.*, 2007), was unable to properly depict all of the micro-topographic features. The magnitude of the resultant flattening is evident in the maximum absolute errors recorded in the sample fields (1.67 m, 1.53 m, and 2.36 m for fields 1, 2, and 3, respectively).
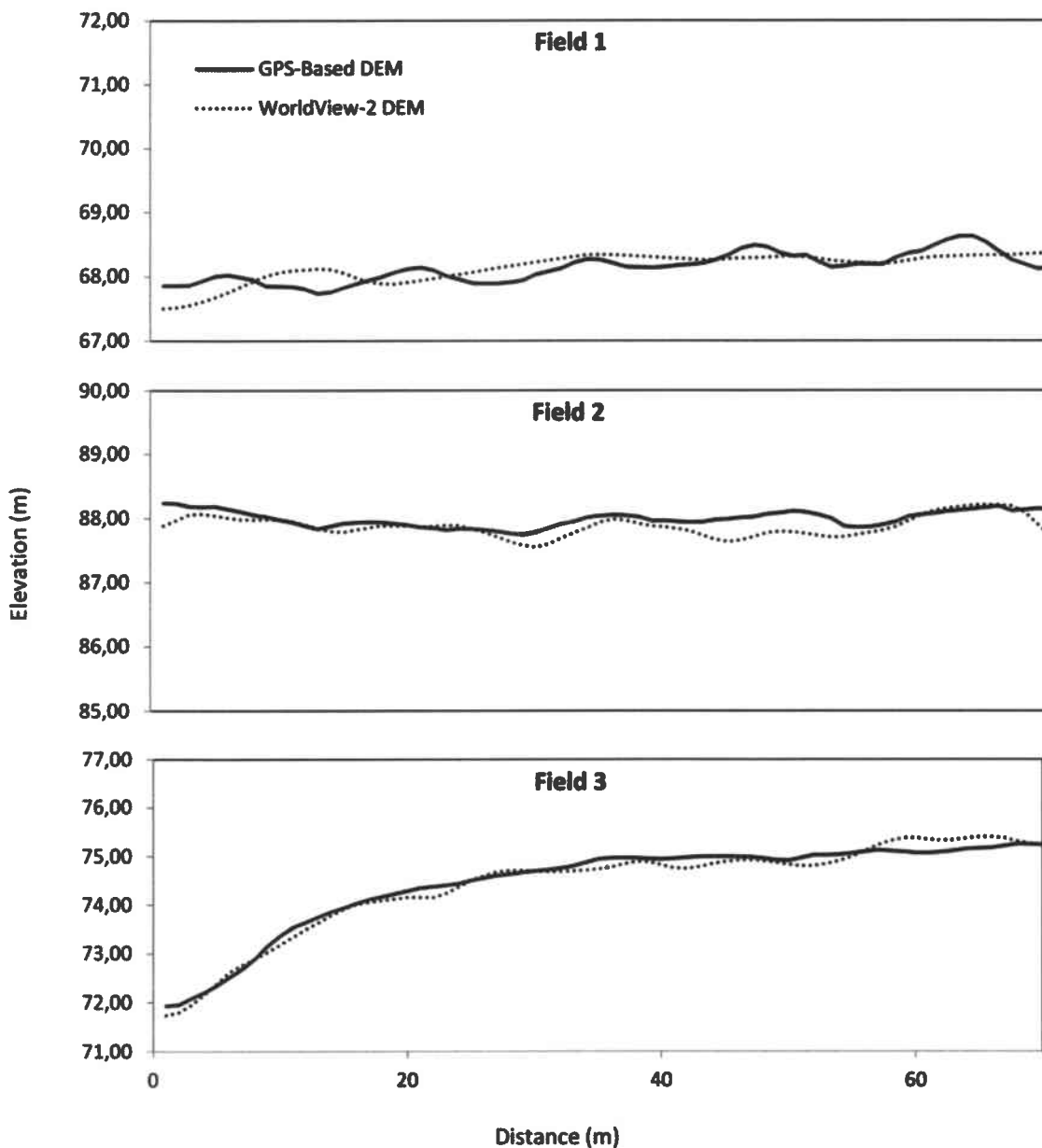
Figure 5.4: Transverse elevation profiles of the sample fields.

It is important to note that at the time the stereoscopic pair was acquired (during the second week of April 2012), there were still snow patches in the study area. The snow was present mostly in depressions and drainage channels. Figure 5.5 shows the snow present in Field 3 (the white patches on the ground), and the hatched polygons where LE90 errors are greater than 0.36 m. Certainly, snow accumulation is one of the causes that influenced the extraction of elevation information.
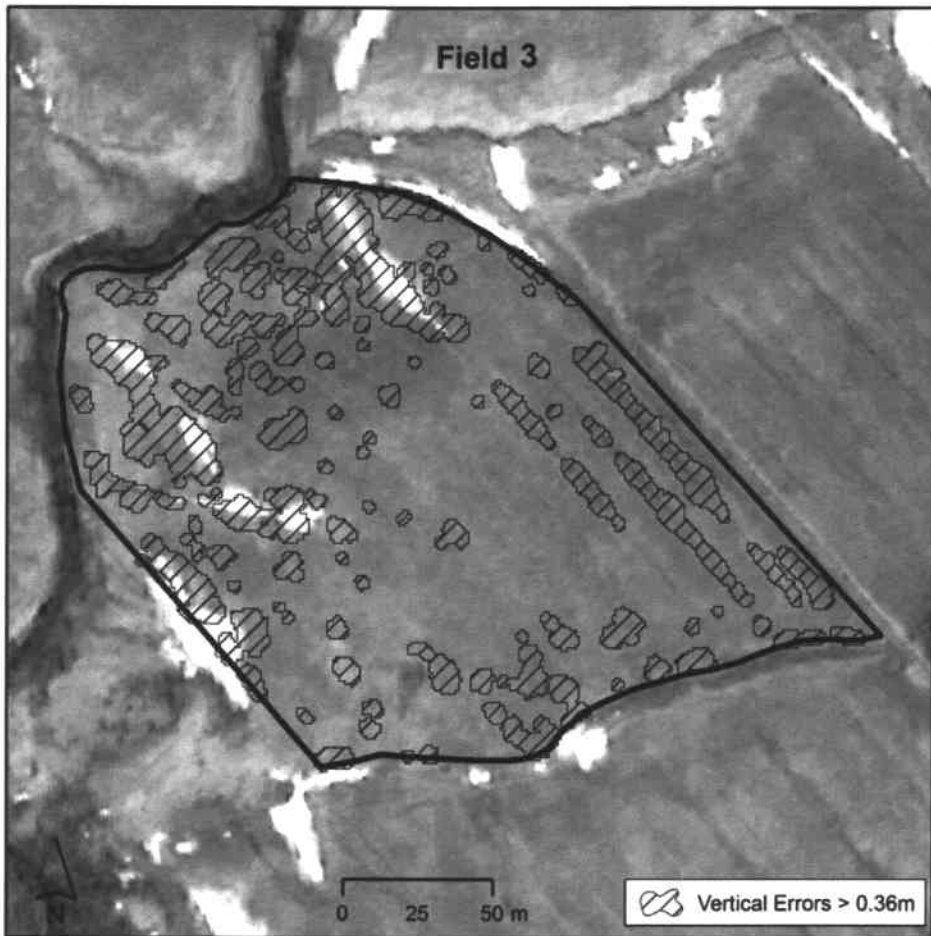
Figure 5.5: Spatial distribution of snow patches and vertical errors on Field 3.

Furthermore, although the vertical accuracy metric is useful, this metric cannot be taken to express the overall performance of the WV-2 DEM in the study area. Our ground-truth check was performed only on agricultural, untilled fields. As Reinartz *et al.* (2010) have suggested, further research using different land cover types and probably different methodologies are needed in order to fully assess the ability of the WorldView-2 satellite to depict elevation in complex landscapes, including forested and urbanized areas. As demonstrated by the metrics calculated for the present study, the vertical precision of the elevation data in the satellite-derived DEM is less than 1 meter, which may be accurate enough for environmental modelling at regional scales. However, at local (field) scales, the inability of the DEM to pick up micro-topographic details could lead to erroneous results. To overcome this problem, reconditioning

42

methods may need to be applied. For example, AGREE, an algorithm incorporated into ArcHydro, modifies DEMs by imposing vector features such as channels and streams to ensure better surface hydrological analysis, especially in the calculation of flow direction and flow accumulation (Hellweger, 1997).

5.3.2 Geomorphological and Drainage Variables

Table 5.5 summarizes the comparison statistics of the geomorphological and drainage variables: terrain depressions, terrain slope, and runoff flow paths. By analysing the relative errors of each quality indicator, we were able to assess the performance of the satellite elevation model at extracting these variables. We selected the relative error e (Eq. 5.2) and its mean absolute value $|e|$ to express the change of each quality indicator in each sample field. All the error metrics are expressed in percentage to ease interpretation.

Table 5.5 : Comparison statistics (terrain depressions, slope, flow paths) between the WV-2 DEM and the GPS-derived DEM for the three fields.

Hydrologic Variables	Field 1			Field 2			Field 3			$|e|$
	GPS	WV-2	e	GPS	WV-2	e	GPS	WV-2	e	
Depressions										
Total Area (m²)	5117	9514	*86%*	1486	2206	*48%*	838	1513	*81%*	72%
Non-Overlapping Area (m²)		3331	*65%*		941	*63%*		726	*87%*	72%
Slope										
Longitudinal Slope (%)	0.3	0.3	*0%*	1.0	1.0	*0%*	5.2	5.1	*-2%*	1%
Mean Slope (%)	3.3	2.5	*-25%*	5.23	6.1	*-54%*	12.9	13.3	*3%*	27%
Maximum Slope (%)	13.9	12.1	*-13%*	26.52	33.9	*-48%*	62.8	65.5	*4%*	22%
Flow Paths										
Mean Length (m)	40	13	*-67%*	23	12	*-46%*	20	14	*-28%*	47%
Maximum Length (m)	173	69	*-60%*	164	69	*-58%*	139	66	*-53%*	57%
Total Length (m)	2994	2629	*-12%*	1062	833	*-21%*	2846	2290	*-20%*	18%

First, terrain depressions were analyzed. This variable was the most difficult one for the satellite-derived elevation model to detect. For this assessment, we compared both the total area detected as land depressions in the two DEMs and the non-overlapping area between them. While the total area expresses the quantity of terrain surface that was detected as depressions, the non-overlapping area represents the spatial disparity between the areas detected in the two DEMs, making this a quality indicator of the discrepancy between the DEMs. In both cases, these calculations produced mean absolute errors as high as 72%, demonstrating the difficulty of using the WV-2 DEM to detect land depressions. Despite these unpromising results, it may be

possible to obtain good characterization of terrain depressions using satellite stereoscopic pairs, for instance, by exploiting spectral information to calculate terrain wetness indices. Such techniques, beyond the scope of this paper, are part of the complementary digital image processing techniques available in remote sensing.

Next, terrain slope, expressed here as percentage rise, was analysed. This variable is widely used for spatial modelling (for example, in rainfall-runoff models) and as a component in erosion assessment and of the Universal Soil Loss Equation (e.g., Nigel *et al.* (2013)). The longitudinal slope for each field was calculated over the length of the field, as shown by the arrow in Figure 5.2. There was a little variation (1%) between the two elevation models for the longitudinal slope, showing that the satellite model was able to correctly represent the general slope of an agricultural field. However, we found that the WorldView-2 DEM had difficulties estimating mean and maximum slopes, with mean absolute errors of 27% and 22%, respectively. On rolling terrain (Field 3), slope calculation performed well, with small errors of 3% and 4% in the mean and maximum values (in contrast to flatter fields). In general, the satellite-derived DEM underestimated slopes, confirming the spatial pattern found in the transversal profiles (Fig. 5.4), where a loss of local vertical details can be seen in the WorldView-2 model.

For runoff flow paths, the mean, maximum, and total lengths of the surface drainage pathways were calculated. The high relative errors obtained indicate that the WV-2 DEM also underestimated this variable. The total length calculation had the best overall performance, with 18% relative error, suggesting that WV-2 DEMs may have utility for deriving composite hydrologic variables such as drainage density, which is commonly used in spatial hydrologic modelling. By contrast, as illustrated in Figure 5.6, the WV-2 DEM was unable to accurately determine either the location or the length of flow paths. Such information is necessary to understand the internal hydrologic configuration of a field and design surface drainage structures such as inlet and drainage wells (Beaulieu *et al.*, 2007). To evaluate quantitatively the representation of flow paths, we used two indicators, namely, (1) the drainage outlet and (2) the drainage area of the flow path. For each indicator, relative error (e) and mean absolute relative error (|e|) were calculated for each side of the field (northwest, southeast, northeast, and southwest).
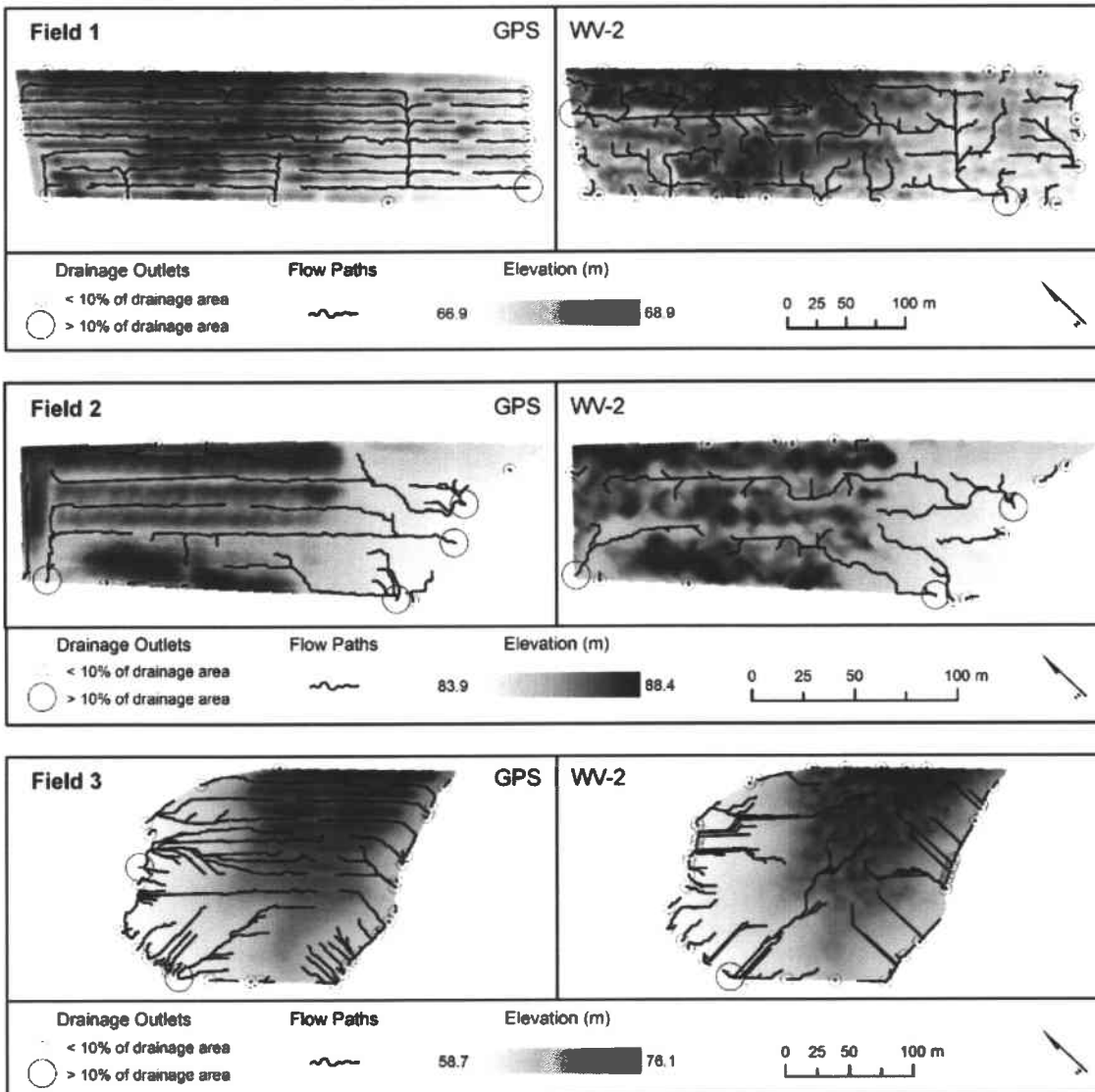
Figure 5.6: Elevation, runoff flow paths, and drainage points for the satellite- and GPS-based DEM for each field. Flow paths are shown as black lines, and drainage outlets are represented as two classes: those with a total drainage area of (i) less than 10% and (ii) more than 10% of the field area. A flow accumulation threshold of 100 cells (i.e., 100 m²) was used to extract the flow paths.

For the drainage outlet indicator, the variable used was the number of drainage outlets per side of the field (Table 5.6). This indicator shows a high mean absolute error of 76%, with the WV-2 DEM mostly overestimating the number of drainage outlets per side of each field. In line with the other indicators and variables analysed, the higher the longitudinal slope, the better the

performance of the WV-2 DEM, with relative error ranging from 111% in Field 1 to 43% in Field 3.

Table 5.6 : Number of drainage outlets derived per side of each field for the flow paths extracted from the GPS- and the WV-2–based DEM (sides with the highest slope are shown in *italics*).

Side	Field 1			Field 2			Field 3		
	GPS	WV-2	e	GPS	WV-2	e	GPS	WV-2	e
Northwest	3	5	67%	1	2	100%	12	14	17%
Southeast	7	4	-43%	3	4	33%	16	15	-6%
Northeast	3	7	133%	2	5	150%	2	5	150%
Southwest	4	12	200%	6	5	-17%	3	3	0%
|e| for each field			111%			75%			43%
Mean |e|					76%				

The drainage area indicator, which represents the cumulative area drained towards an outlet, also presented a high overall relative error (90%, Table 5.7). Similar to the general trend of better performance of the WV-2 DEM in locations with steeper slopes, sample Field 3 had the lowest error (19%).

Table 5.7 : Total drainage surface area (m^2) per side of each field for the flow paths extracted from the GPS- and the WV-2–based DEM (sides with the highest slope are shown in *italics*).

Side	Field 1			Field 2			Field 3		
	GPS	WV-2	e	GPS	WV-2	e	GPS	WV-2	e
Northwest	8085	12969	60%	375	2056	448%	18158	16733	-8%
Southeast	24908	4567	-82%	8197	7352	-10%	10642	11659	10%
Northeast	466	1360	192%	559	676	21%	1862	1397	-25%
Southwest	9680	24948	158%	5658	3964	-30%	795	1051	32%
|e| for each field		123%			127%			19%	
Mean |e|					90%				

5.3.3 General discussion

The performance of the WV-2 DEM in representing field slopes is better in steep terrain (Field 3) than flat or gentle terrain (fields 1 and 2). The smaller relative errors obtained in the former show the potential applicability of the WV-2 DEM for environmental and hydrologic modelling in such terrain. Multi-temporal Very High Spatial Resolution (VHSR) WV-2 DEMs could be highly useful in those parts of the landscape that usually have the steepest slopes, such as riverine and riparian areas. In such areas, the slopes usually go from moderate to high, often within a short distance, and the interactions between agricultural land and water streams must be monitored regularly to protect and improve the quality of aquatic and environmental resources. Moreover, it is important to note that WorldView-2 imagery offers eight multispectral bands and elevation data using a single data source. This fact reduces data acquisition costs to approximately 1.5$/ha. Using other data sources these costs might increase to 1.3$/ha only for the spectral information (aerial photography), and from 0.75 to 4.0 $/ha, for the elevation information (LiDAR), depending upon the point density desired.

The overall performance of the WV-2 DEM in correctly representing terrain depressions of the three fields was 72% (mean absolute relative error $|e|$). Field 2, which is characterized by gentle slopes (mean ~6%), had the lowest $|e|$ (48%). This means the WV-2 DEM may be better at detecting terrain depressions in intermediate terrain than flatter or steeper terrain. Overall, however, the performance of the WV-2 DEM in extracting terrain depression information was unsatisfactory. The multispectral imaging capabilities of the satellite may offer an alternative means to extract more accurate depression data, as such regions are usually characterized by higher soil water content, a parameter that can usually be detected in the spectral information of the images (Lyon *et al.*, 2003).

The flow paths of surface runoff in vector format were used to extract three indicators, namely, mean length, maximum length, and total length of flow paths. Only total length performed well in all sample fields, showing a mean absolute relative error ($|e|$) of 18%. This variable can be used to extract other composite variables, such as the drainage density (useful as an indicator of landscape dissection) or runoff potential. The other two flow path indicators, mean length and maximum length, had $|e|$ of 47% and 57%, respectively, confirming that the picture of the internal connectivity and distribution of runoff channels extracted from the satellite DEM is not reliable at this scale (i.e., inside the field).

The WV-2 DEM also performed poorly in drainage outlet analysis, producing a mean absolute relative error ($|e|$) of 76% across the three fields, with Field 3 having the lowest value (43%). The overall performance of the WV-2 DEM was lower in drainage area extraction than drainage outlet extraction. However, while the drainage area indicator shows a mean absolute error of 90% across the three fields, the lowest value recorded (Field 3, 19%) was better than the 43% recorded for drainage outlet extraction. This might suggests that drainage area information extracted from WV-2 DEMs is useful as a parameter in environmental modelling in terrain with a slope generally >5%.

Vertical error metrics such as RMSE rely on error propagation theory, where it is assumed that vertical errors have a normal distribution, a condition that is not always found in elevation data (Liu *et al.*, 2012b). This approach ignores the already-proved influence of land morphology in RMSE calculations (Wilson, 2012) and thus reduces the usefulness of RMSE as a proxy for the quality of micro-topography and surface hydrologic variables extracted.

The disparities between the drainage outlet and drainage area indicators extracted and the actual parameters of the sites can be seen in Figure 5.6. Both indicators show their best performance in Field 3, revealing that the extraction of geomorphological and drainage parameters is better in steeper terrain than in flat terrain (except probably for the extraction of terrain depressions, which as discussed above, was better in Field 2). Figure 5.7 shows the global mean absolute relative errors (by field) and the corresponding longitudinal slope. The global mean absolute relative error (MARE) of a field was calculated using the mean of the absolute errors of the geomorphological and drainage variables extracted from each field. We found an inverse proportional relationship between MARE and longitudinal slope, i.e., fields with a low longitudinal slope had an overall higher MARE in all hydrologic variables extracted. Field 3 had the lowest global MARE (37%). Indeed, some variables performed well in Field 3, with relative errors of less than 20%, suggesting that WV-2 DEMs may be useful in such terrain settings. It is advisable that more research and in-situ verifications must be done to define more precisely the advantages and limitations of satellite DEMs.
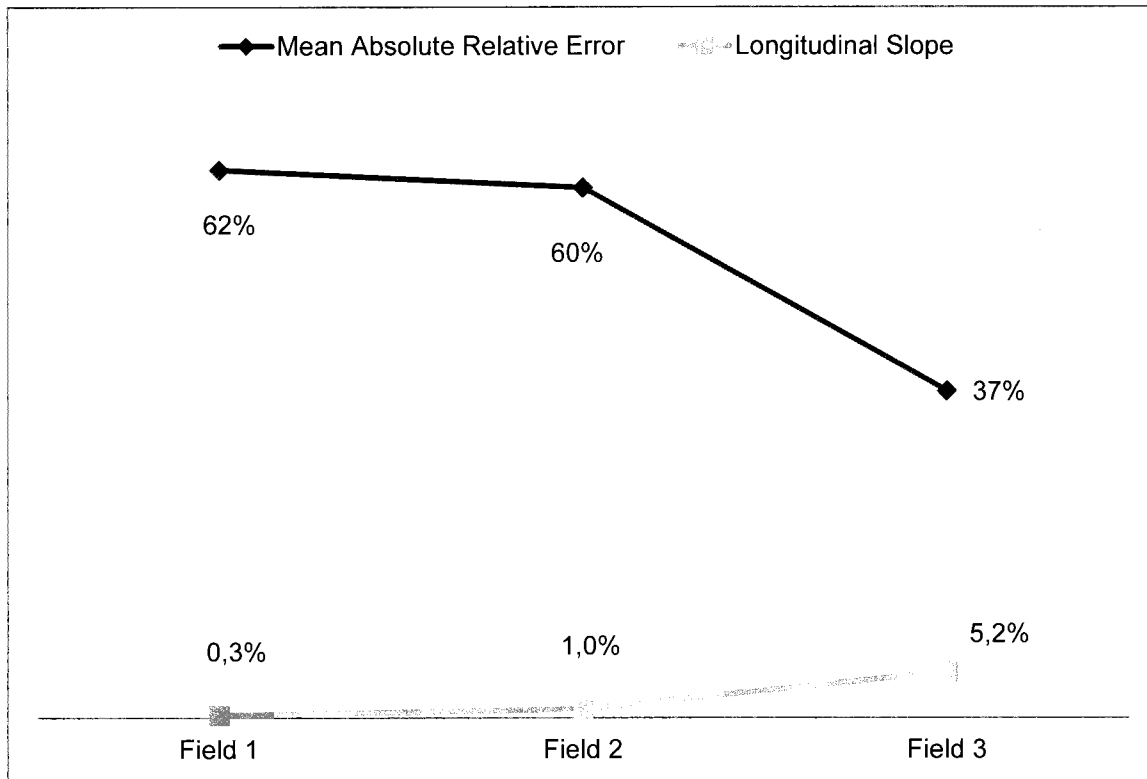
Figure 5.7: Mean Absolute Relative Errors and longitudinal slopes of sample fields.

The satellite-derived elevation model had difficulty extracting accurate surface hydrology features in flat terrain, mainly due to technical issues such as satellite geometric and spectral limitations, and automated DEM production algorithms (Callow *et al.*, 2007, Nardi *et al.*, 2008). Further research comparing geomorphological and drainage variables and terrain complexity indices, as suggested by Huaxing (2008), needs to be done to define more meaningful accuracy metrics to assess the quality of micro-topographic hydrologic variables extracted.

To better understand the influence of the particular algorithms used in available software, a number of studies have compared the performance of different programs when calculating parameters for hydrologic modelling (Endreny *et al.*, 2001, Wilson, 2012, Zhang *et al.*, 1999, Zhou *et al.*, 2004). Such comparisons are beyond the scope of this study, however; our primary goal was to assess the relative accuracy of the various geomorphological and drainage parameters calculated, not to determine the best methods available to compute such parameters.

WorldView-2 DEMs offer a practical and fast means to obtain accurate digital elevation models at high spatial resolution. Elevation accuracy metrics such as the root mean square error and the linear error at the 90th percentile are currently the standards upon which commercial remotely sensed elevation models are based, but further research must be done to incorporate new metrics for assessing the quality of micro-topographic representation in such elevation models.

At agricultural field scales, even with a vertical accuracy of one metre in a satellite-derived DEM product, not all geomorphologic and drainage variables were correctly extracted, demonstrating that there is a discordance between vertical accuracy metrics and the quality of these variables. Overall, for the three fields, the variables that were most accurately extracted were *total length* of runoff flow paths (18%), *maximum slope* (22%), and *mean slope* (27%). These three variables, in terms of hydrological modelling, are not relevant when compared to drainage pathways and drainage outlets. Using Field 3 as a proxy for terrain with rolling and higher slopes (>5%), the variables that presented potential for use were *mean slope* (3%) and *maximum slope* (4%). The variables *drainage area* (19%) and *total length* of runoff flowpaths (20%) also had comparatively good performances, making them potentially useful for representing the field as a whole, but not for micro-topographic representation. Steeper terrain is generally found in hilly and mountainous regions, but steep slopes can also be found in riverine areas of low-relief watersheds, such as the La Chevrotière River Basin. Consequently, a WorldView-2 DEM can be used, with the limitations explained previously, as a decision-making tool by watershed organizations, government offices, and landscape planners. Satellite-derived DEMs might help characterize, monitor, and preserve the natural resources of riverine areas.

The results produced by satellite-extracted DEMs, in hydrological studies at field scales, can vary widely, depending on the weights of the topographic variables in the hydrological modelling, but they follow the trends found in several studies previously cited. For example, Kenward *et al.* (2000) found that even minimal variations in slope can lead to predictions of mean annual runoff volumes in a river basin from 0.3% to 7% higher than expected. Most of the problems found in the results produced by the WorldView-2 DEM are quite similar to those found when comparing coarse resolution DEMs: underestimated slopes and flow paths lengths, and overestimated depression areas, drainage area and outlets (Erskine *et al.*, 2007, Zhang *et al.*, 1994), that is:

- It is important to note that slope underestimations in the satellite DEM affect the overland and subsurface flow velocity and runoff rate, as well as solar irradiation. This topographic variable is one of the most used in environmental modelling such as in the universal soil

loss equation to quantify sheet and rill erosion by water, or to evaluate potential evapotranspiration, which plays a major role in a catchment's water budget.

- Flow path length underestimations changes the erosion rates, sediment yield, and time of concentration.
- Drainage area overestimations increase the predicted runoff volume.
- Drainage outlets overestimations degrade our capability to find the right place to take action to protect from erosion
- An excessive overestimation of land depressions might have implications in hydraulic works planning at farm level
- Micro-watershed area is a parameter that reflects the surface runoff area at a given point
- Combined variables such as the topographic index, used for representing soil moisture and water concentration, with underestimated slope values and overestimated drainage areas, will increase, predicting more humid surfaces of what is available in reality.

Spectral information is one of the most important features that separate a very high spatial resolution satellite like WorldView-2 from other options for the extraction of digital elevation models. Some of the weaknesses of the stereoscopic extraction of elevation can be overcome by developing complementary methods to extract information using both spectral and stereoscopic information. Our examination of the extraction of hydrologic variables at field scales confirmed the limitations of satellite DEMs in flat terrain, but it also showed that they have potential usefulness in terrain with steeper slopes, where better results were obtained. In order to exhaustively exploit the potential of very high spatial resolution stereoscopic satellite imagery for surface hydrologic variable extraction and environmental modelling, further research is needed using alternative flow routing algorithms, land cover extraction methods, spectral information, and DEM modification techniques.

5.4 Conclusions

This study found a global vertical accuracy of 0.45 m in a WorldView-2 DEM product when assessed against ground truth GPS-RTK high-density and high-precision point data sets over three agricultural fields with nearly level (0–0.5%), gentle (0.5–2%), and rolling (5–10%) topographic slopes. These results confirmed the potential of WV-2 stereoscopic image pairs to extract elevation information at high spatial (1-m) resolution. For the extraction of geomorphologic and drainage variables, the WV-2 DEM performed better on the field with rolling slopes (5–10%), extracting quality indicators such as total length of flow paths and drainage area with relative errors lower than 20%. This suggests that satellite-derived DEMs have potential for use in environmental modelling applications in areas with rolling or steep slopes. However, the results also indicate some limitations of the WV-2 DEM in the extraction of terrain slope, drainage outlets, and terrain depressions in areas of flatter slopes (<5%). Ground-truth validation, including bigger, more topographically-diverse sampling areas are needed in order to validate and expand scientific knowledge in these areas.

5.5 Acknowledgments

6 RIPARIAN STRIP EFFICIENCY ASSESSMENT IN AGRICULTURAL LANDSCAPES USING STEREOSCOPIC VERY HIGH SPATIAL RESOLUTION SATELLITE IMAGERY

Julio Novoa[a], Karem Chokmani[a]

[a] *Institut National de la Recherche Scientifique, Centre Eau Terre Environnement, 490 rue de la Couronne, Québec (QC) G1K 9A9, Canada*

Abstract

Riparian strips are used worldwide to protect riverbanks and water quality in agricultural zones because of their several environmental benefits. A metric called the Riparian Strip Quality Index, which is based on the percentage area of riverine vegetation found on the riparian strip, is used to evaluate their ecological condition. This index could be considered an indicator of the potential capacity of riparian strips to filter sediments, retain pollutants, and provide shelter to terrestrial and aquatic species. Thus, in order to know if a riparian strip is truly efficient in agricultural lands, which means that it is fulfilling those ecological functions, it is necessary to understand their ability to intercept surface runoff. The latter is the major cause of water pollution and erosion in these productive areas. Besides vegetation coverage, topographic and hydrologic parameters must be included to model the intensity and spatial distribution of runoff streamflow at local scales. The geospatial information used to assess the ecological efficiency of riparian strips was extracted from very-high-spatial-resolution WorldView-2 satellite imagery. This information was then processed using current geospatial techniques such as object-based image analysis and was used to develop a Riparian Strip Efficiency Index. The results show that this index might be used to assess the efficiency of riparian strips, which will enable land managers to monitor changes occurring over time, identify priority areas for restoration activities. This, in turn, might ensure optimal allocation of private or public funds towards the most inefficient and threatened riparian strips.

6.1 Introduction

Riparian strips are well known for their many ecological functions that help in the protection of riverine landscapes and their biota (Boutin *et al.*, 2003, Naiman *et al.*, 1997). These strips, when vegetated, serve to protect water quality, controlling its temperature (Janisch *et al.*, 2012), and their filtering capabilities reduce nonpoint source pollution in agricultural areas (Parn *et al.*, 2012, Sahu *et al.*, 2009). They have also been found effective to prevent erosion caused by water runoff (Duchemin *et al.*, 2009) and to sequestrate large amounts of carbon when covered by trees (Fortier *et al.*, 2010). They also play a key role in preserving biodiversity when working as wildlife corridors (Borin *et al.*, 2010).

Worldwide, riparian habitats are threatened by natural and anthropogenic activities that have gradually fragmented and, in some areas, almost eliminated them from urban and agricultural landscapes (Charron *et al.*, 2008, Saint-Jacques *et al.*, 1998, Vought *et al.*, 1995). In the province of Quebec, the Ministry of Sustainable Development, Environment, Fauna, and Parks (MDDEFP, for its French acronym), through environmental laws and regulations, protects these fragile habitats, establishing standards for the width of the strips according to land cover zoning and terrain slope. Widths from ten to fifteen meters are specified in most land cover zones, but in agricultural regions the protected widths range from three to four meters (Mddefp, 2002, Mddefp, 2005).

The Mddefp (2008) has adopted a metric called the Riparian Strip Quality Index (IQBR, for its French acronym), drawing on the recommendations of Saint-Jacques *et al.* (1998), to evaluate the ecological condition of riparian habitats and their impact on the integrity of aquatic environments. This index is based on the correlation found between the ecological conditions of benthic and fish communities across many watersheds and the different types of riparian vegetation. The IQBR is widely used to create ecological portraits of watersheds, especially for further development of water protection plans. Basically, the index is a weighted sum of land cover area percentages in the riparian strip, with greater weight given to arboreal vegetation and lesser to bare soils. The MDDEFP uses an operational, in-situ technical protocol to characterize riparian strips and evaluate the IQBR. However, methodologies executed in the field are time-consuming, subjective, difficult to replicate, and very demanding in terms of human and material resources, facts that make it very difficult to monitor on regular basis the evolution of the ecological conditions of riverine lands (Ashraf *et al.*, 2010).

Since their inception several decades ago, geographic information systems and remote sensing techniques have been used for the characterization, analysis, and monitoring of natural resources, providing scientists with valuable information to understand land surface processes (Basnyat *et al.*, 2000, Goetz, 2006, Narumalani *et al.*, 1997). In 1999, stereoscopic satellite imagery, with pixel sizes of less than one meter have become available, offering the possibility of a "one-stop" solution to obtain multispectral and ground elevation information on regular basis and at very high spatial resolution (Gu *et al.*, 2010, Johansen *et al.*, 2007). Such imagery has the potential to supplement or replace aerial photographs or airborne multispectral imagery as a source of multispectral information, and it is available worldwide with very short revisit times

(Ghosh *et al.*, 2014, Goetz *et al.*, 2003). Object-based image analysis is considered a proven alternative to per-pixel–based classifiers to extract land cover coverage data from this highly heterogeneous imagery (Gergel *et al.*, 2007, Johansen *et al.*, 2010, Tormos *et al.*, 2011). This technique relies on the segmentation of groups of pixels to create objects (i.e. polygons) and work with them at different scales to extract geospatial information from a landscape. Working with objects enables spectral, geometric, thematic, and topological information to be utilized, creating a richer framework from which to extract geographic information (Benz *et al.*, 2004, Hay *et al.*, 2005).

Some research has also been done on the usefulness and efficiency of riparian strips and the factors that influence their ability to protect water quality by reducing and preventing nonpoint source pollution (Hickey *et al.*, 2004, Lin *et al.*, 2002, Liu *et al.*, 2008). Briefly, the efficiency of such strips is known to be proportional to the size of the transported particles, the width of the strips, and the concentration of sediments but inversely proportional to the slope of the terrain and the magnitude of streamflow (Duchemin *et al.*, 2004, Gumiere *et al.*, 2011). In addition, as Lowrance *et al.* (1997) have shown, the hydrologic configuration of streams, riparian strips, and agricultural fields determines the efficiency of the surface water runoff filtering and sediment retaining functions of the riparian strips. Given their potential to affect the ecological functions of riparian strips, terrain slope and water runoff are the most important topographic and hydrologic variables (Piechnik *et al.*, 2012). The full range of these parameters is rarely integrated into farm management practices (Aarons *et al.*, 2013), and the fact that surface runoff in agricultural areas is concentrated in channels or ditches long before approaching the riparian strip and water streams (Hosl *et al.*, 2012) means that a riparian strip efficiency metric is widely required. Surface runoff variables can be used to model the efficiency of such strips, which is maximized when water runoff is homogeneously distributed along the strip, enabling it to filter and retain the greatest possible proportion of the sediments and pollutants coming from highlands (Duchemin *et al.*, 2004, Gumiere *et al.*, 2011).

Generally, hydrological modeling using gridded digital elevation models (DEM) has mostly been done at the watershed scale (Hage *et al.*, 2012, Hosseinzadeh, 2011, Rezak *et al.*, 2012). To date, this approach has not been used to support operational, local methodologies to assess the efficiency of riparian strips at agricultural field scales, mainly because of the coarse spatial resolution and vertical accuracy of the outdated digital elevation models commercially available.

Thus, most riparian strip assessments have focused on extracting land cover information and evaluating ecological condition using field campaigns, complemented in some cases by aerial photographs or light detection and ranging (LiDAR) data sets, to characterize these habitats (Congalton *et al.*, 2002, Gergel *et al.*, 2007, Yang, 2007a). However, current satellite-derived spectral and altitudinal information offers better spatial resolution (<1m) and vertical accuracy (±1m), and now presents an attractive alternative for the rapid, periodic extraction of land cover, geomorphological and drainage information to assess the ecological quality and efficiency of riparian strips at local scales (Novoa *et al.*, 2013).

The current study focuses on the development of a riparian strip efficiency index assisted by stereoscopic satellite imagery at very high spatial resolution in order to help land managers and farmers better understand and manage their riparian strips and thus protect the environmental quality of watersheds.

6.1.1 Study area

The La Chevrotière River basin is located in the regional municipality of Portneuf, 60 kilometers west of Quebec City, on the north shore of the Saint Lawrence River (Fig. 1). There are two main urban centers within the basin, St-Marc-dès-Carrières and St-Gilbert, which together contain approximately 3,100 inhabitants. The watershed covers an area of 108 km^2, and its topography ranges from flat to undulating in a landscape covered mainly by forests (60%) and agricultural land (34%). The La Chevrotière River, which is composed of two main branches, runs 29 km and flows out to the Saint Lawrence River. Slopes in the watershed range from 0% in agricultural and urban areas to more than 8% in riparian areas. The region receives 1,152 mm of precipitation per year with 932 mm in liquid precipitations. During April, when the snow starts to melt, soils in the basin become saturated and there is an increased risk of erosion induced by surface water runoff dynamics. This is one of the problems that healthy riparian strips can help to mitigate.
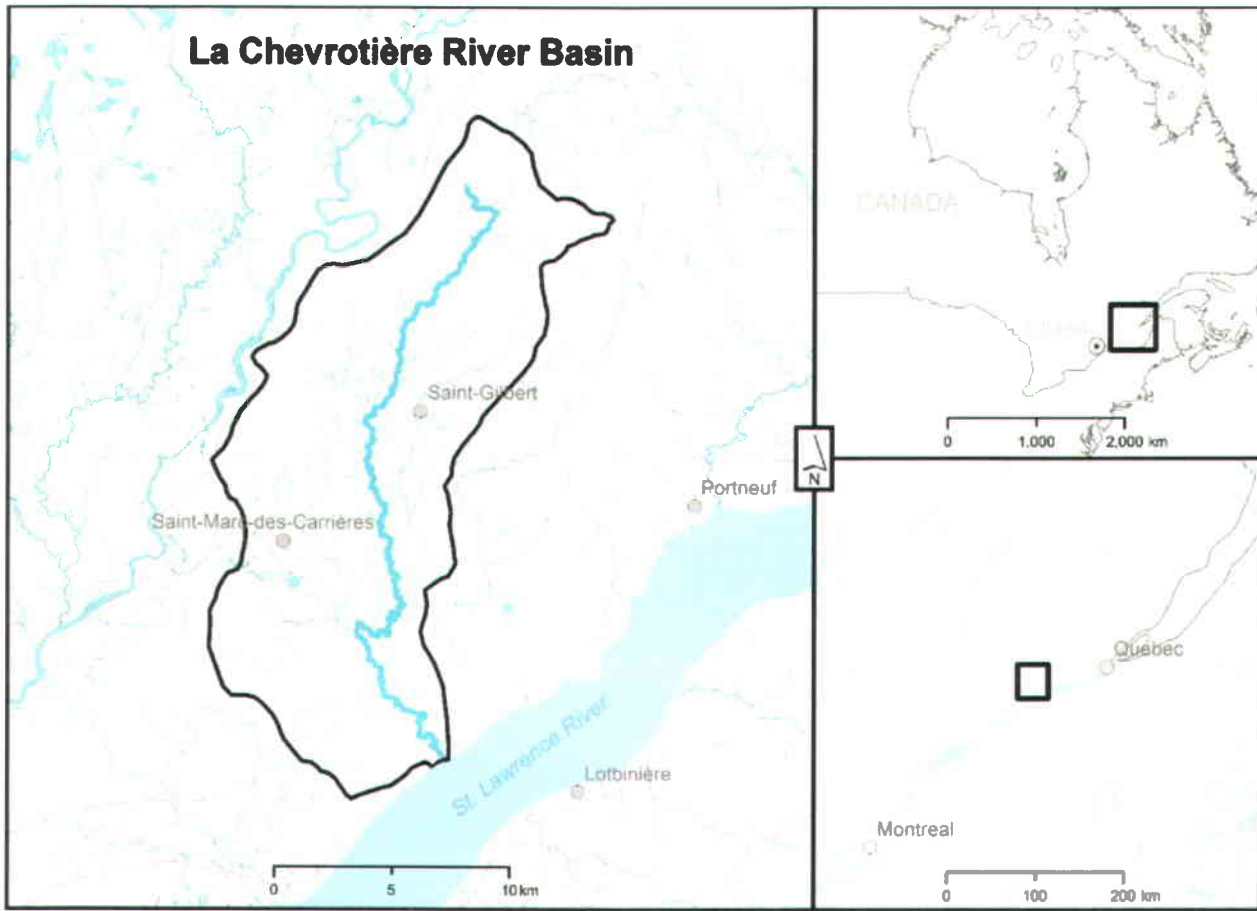
Figure 6.1 : La Chevrotière River Basin, located between Montreal and Quebec City, in the province of Quebec, Canada

6.2 Methods

The methodology takes advantage of remotely sensed information at very high spatial resolution and the analytical capabilities of object-based image analysis and geographic information systems to evaluate the ecological quality and efficiency of riparian strips in fulfilling their ecological functions in a watershed (Fig. 2). Two main input data sets are used: land-use information collected during fieldwork and satellite-derived information (multispectral information and the digital elevation model). The final result is a geospatial data set that contains polygons representing every riparian strip, along with their ecological quality (IQBR) and efficiency (RSEI).
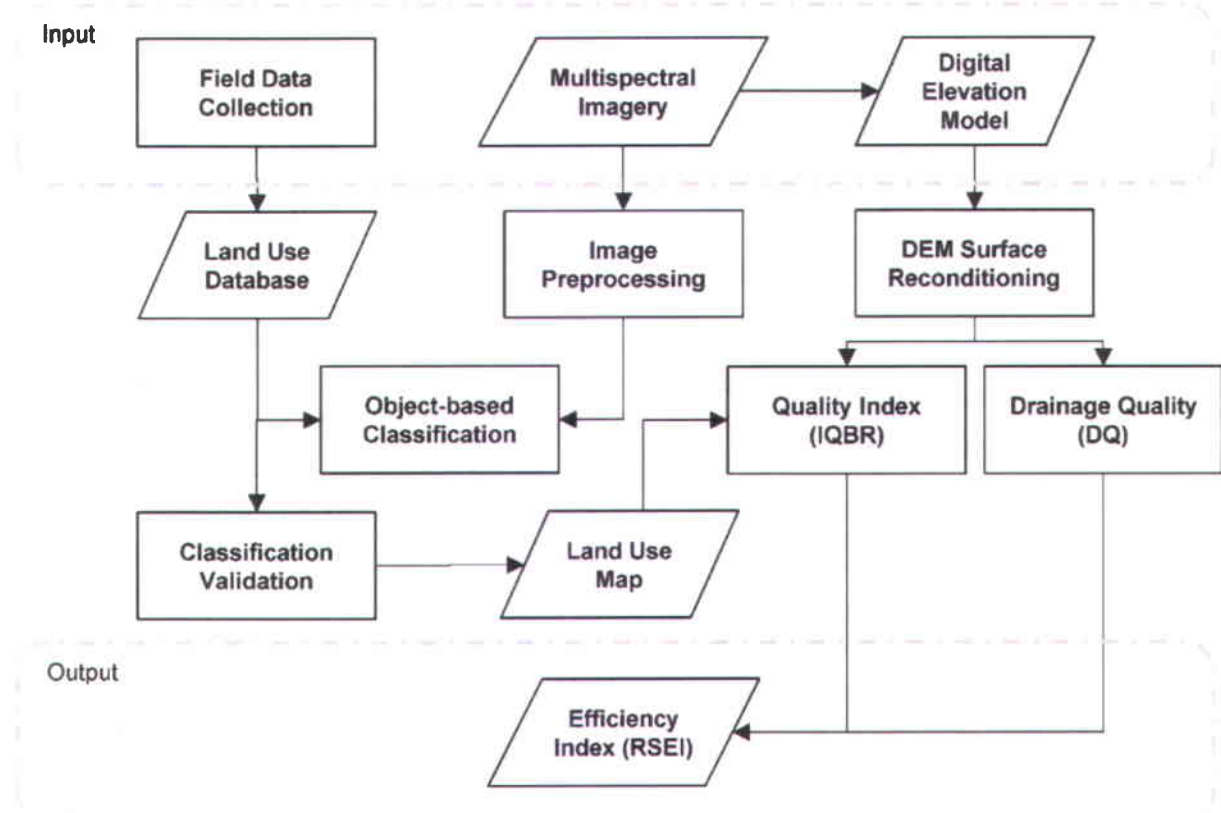
Figure 6.2 : Flowchart of the approach used to evaluate the ecological efficiency of riparian strips in agricultural areas.

6.2.1 Field data collection

A fieldwork campaign was carried out during summer 2011 to evaluate the ecological status of the riverine zones of the watershed. Using stratified random sampling, 80 locations were evaluated in-situ using the technical protocol developed by the Mddefp (2008). The stratified sampling took into account the Strahler Stream Order and the land-use zoning of the study area. Due to accessibility problems, most of the samples were collected in agricultural zones, which is why future comparisons and validations were only used for agricultural lands. It is also important to mention that riparian strips of one hundred meters length were sampled, instead strips of five hundred meters as stated in the MDDEFP methodology. This decision was made because of difficulties faced in the field when attempting to assess land cover area percentages on riverbank segments longer than 100 meters. The longer the segment, the more subjective the visual assessment became. Thus, land cover and topographic information was collected in-situ

from both riverbanks through direct observations. A geographic information system was used to store and analyze the collected information, enabling us to combine GPS coordinates, land cover observations, photographic records, and slope measurements done in the field.

6.2.2 Image acquisition and preprocessing

Two WorldView-2 satellite images were acquired for this project. The images were taken in summer 2011 and spring 2012 in order to capture the spectral variation due to vegetation seasonality. Each image included data from eight spectral bands at 2-meter spatial resolution and one panchromatic band at half-meter spatial resolution. From the spring image, the provider extracted a digital elevation model of 1-meter spatial resolution and 1-meter vertical accuracy using automated image matching algorithms.

In order to extract accurate land cover information, some preprocessing was performed on both satellite images to improve their spectral information and correct their geometry. All preprocessing steps were performed on the two images independently. An atmospheric correction was performed using the algorithm ATCOR2 (Richter, 1997). Afterward, using six high-precision (±0.1m) GPS control points, the atmospherically corrected images were orthorectified, achieving a horizontal precision of less than one meter for both images. Finally, to improve the spatial resolution of the multispectral bands, the images were pan sharpened using the algorithm PANSHARP2 (Zhang, 2002), which preserves spectral characteristics of multispectral channels. As a result, two images were created, each with eight spectral bands at half-meter spatial resolution.

To reduce and synthesize the variability within the eight multispectral bands of each image, the first principal component was extracted (Ghosh *et al.*, 2014), which included more than 90% of the spectral variability of the eight bands of each image (93% for summer 2011 and 97% for spring 2012). Next, the normalized difference vegetation index (NDVI) was calculated for both images, taking advantage of the Red Edge spectral band of this satellite to better discriminate vegetation types (Mutanga *et al.*, 2012). Consequently, a four-band raster file was created (henceforth called the *composite raster*), combining the first principal component and the NDVI of each image. This combination has proven to be effective in extracting riparian vegetation

(Johansen *et al.*, 2007). Following this approach, the two multispectral images were combined into a single raster to reduce file size, spectral complexity, and computing time.

6.2.3 DEM Surface Reconditioning

Even at 1-meter spatial resolution, the satellite-derived elevation model faced problems when modeling micro-topographic details such as terrain depressions or ditches (Novoa *et al.*, 2013). To overcome this problem, the algorithm AGREE was applied to the DEM using a vector data set containing all surface drainage channels (e.g. ditches). This data set was created by digitizing on-screen using the multispectral satellite image as background. The algorithm then imposed these features on the DEM to ensure better hydrologic modeling (Hellweger, 1997).

6.2.4 Object-based Classification

Since the launch of IKONOS, the first commercial, very high spatial resolution optical satellite, in 1999, object-based image analysis has grown to become a mainstream technique used to digitally extract geospatial information (Blaschke, 2010). The software eCognition (Trimble, 2011), used in this research, relies on a multiresolution segmentation algorithm to group similar pixels into geospatial entities called objects. The algorithm creates objects by consecutively merging pixels or existing image objects using a bottom-up approach based on a pairwise region-merging technique (Benz *et al.*, 2001).

It is worth noting that all the following procedures were executed using the composite raster, but only after applying a geographic mask corresponding to a 50-meter buffer around water streams. This geographic fence was considered sufficient as the required width of riparian strips in the study area ranges from 3 to a maximum of 15 meters.

Image segmentation is one of the most important steps in an object-based classification; the parameters used in segmentation are crucial to the accuracy of the outcome (Liu *et al.*, 2012a). The estimation of the optimal scale parameter was carried out using the software module

developed by Dragut *et al.* (2010), which evaluates spatial and spectral variabilities at different scales to detect important changes in the delineation of objects. The scale parameter used was 25, while the shape and compactness parameters were both 0.1. These parameters enabled the creation of elongated objects, as expected in riverine ecosystems. After visual verification, only the first principal component was used to delineate the objects used for the image classification. This approach is supported by the findings of Lippitt *et al.* (2012), who tested the performance of principal components in the object segmentation process.

Once the composite raster was segmented, seven land cover classes were created. Sample objects were then selected using information collected during fieldwork. These samples were used to describe each land cover class using the spectral information derived from the first principal component and the NDVI from both satellites images (Table 6.1). The information collected through these sample objects was then used to perform a feature space optimization analysis. Only statistically representative variables were selected. The sixteen variables, calculated for every object in the composite raster file, were object area, object brightness, spectral skewness, shape index, spectral mean, spectral standard deviation, and spectral maximum difference. The nearest-neighbor algorithm, which assigns objects to a class based on a fuzzy membership value, was used to classify the composite raster.

Table 6.1 : Land cover classes, their training areas, and riparian area percentages.

Land Cover Class	Training Area (m²)	%
Grass	649,211	4.3
Forests	592,120	3.9
Crops	336,484	2.2
Herbaceous	79,688	0.5
Infrastructure	69,316	0.5
Shrubs	50,263	0.3
Bare Soil	44,350	0.3
Total	1,821,431	12.0

6.2.5 Classification Validation

After classifying the composite raster, a validation of the object-based classification was performed. Validation samples (181) at 95% confidence level and 10% margin of error were randomly selected and independently evaluated on screen. The number of validation objects selected for each land cover class was determined by the percentage of objects falling within that classification, as seen in Table 6.2. A confusion matrix, producer's and user's accuracies, and the K coefficient were then calculated to show the degree of agreement between ground truth and the classified land cover (Congalton, 1991).

Table 6.2 : Number of objects produced by the object-based classification, and the number of objects randomly selected for validation

Land cover Class	Classified Objects	%	Validation Objects
Forests	505	29%	52
Grass	391	22%	40
Herbaceous	382	22%	39
Infrastructure	283	16%	29
Shrubs	112	6%	12
Bare Soil	44	3%	5
Crops	39	2%	4
Total	1,756	100%	181

6.2.6 Riparian Strip Quality Index (IQBR)

The IQBR is a measure of the ecological quality of riparian strips, and it is commonly used to create ecological portraits of watershed riparian areas. Calculated using weighted riparian land cover classes (Eq. 6.1), it can also be used as a tool to verify legal compliance and to help land managers monitor changes in riverine habitats. The IQBR is calculated as follows:

$$IQBR = \frac{\sum (\%LU_i \times W_i)}{10} \tag{6.1}$$

where $\%LU_i$ is the land cover area percentage inside the riparian strip and W_i corresponds to the land cover class weighting factor: *forests* (10.0), *shrubs* (8.2), *herbaceous vegetation* (5.8), *crops* (1.9), *grass* (3.0), *bare soil* (1.7), *infrastructure* (1.9), *bedrock* (3.8), and *logging areas* (4.3). This calculation was done automatically in a GIS on 500-m length riparian strips, except in agricultural areas, where riparian strips had the same length as the agricultural fields they went through. The IQBR ranges from 17 (lowest ecological quality) to 100 (highest ecological quality).

6.2.7 Drainage Quality Analysis in Agricultural Zones

In addition to vegetation, topography plays an important role in modeling how riparian strips intercept runoff and retain sediments (Fernandez *et al.*, 2012, Piechnik *et al.*, 2012, Teufl *et al.*, 2013). As Bereswill *et al.* (2013) argue, the width of a riparian strip is not enough to measure the performance of these vegetative filters. Accordingly, in agricultural land, where the landscape is often highly modified through field leveling, by drainage ditches, or hydraulic works, e.g., to boost productivity, the IQBR may be insufficient to precisely depict the efficiency of riparian strips. Consequently, land cover information must be complemented by runoff metrics (flow volume and spatial distribution) to provide land managers and farmers with useful information to take wise decisions regarding riparian habitats, productivity, erosion, and water and soil quality.

Concentrations of surface runoff in riparian strips are commonly caused by a disadvantageous drainage configuration. Several algorithms are available to simulate water distribution and calculate streamflow magnitude in watersheds. The accuracy of these algorithms has been extensively tested when calculating flow direction and flow accumulation using gridded DEMs

(Wilson *et al.*, 2008, Zhou *et al.*, 2002). For this research, we selected the D8 flow routing algorithm (Jenson *et al.*, 1988a), which is one of the most widely used in hydrological modeling because of its simplicity of implementation. The performance of the D8 algorithm is known to be inferior to that of more sophisticated, complex flow routing algorithms, but its results are considered acceptable for the detection of potential streamflow concentration in agricultural fields (Wilson *et al.*, 2007).

Drainage quality (DQ) was calculated individually for each riparian strip, as follows:

$$DQ = \frac{\sum(Drainage_{P75})}{Field\ Area} \tag{6.2}$$

where $\sum(Drainage_{P75})$ is the sum of the areas drained by the extreme outlets, and *Field Area* is the total area of the agricultural field in contact with the riparian strip.
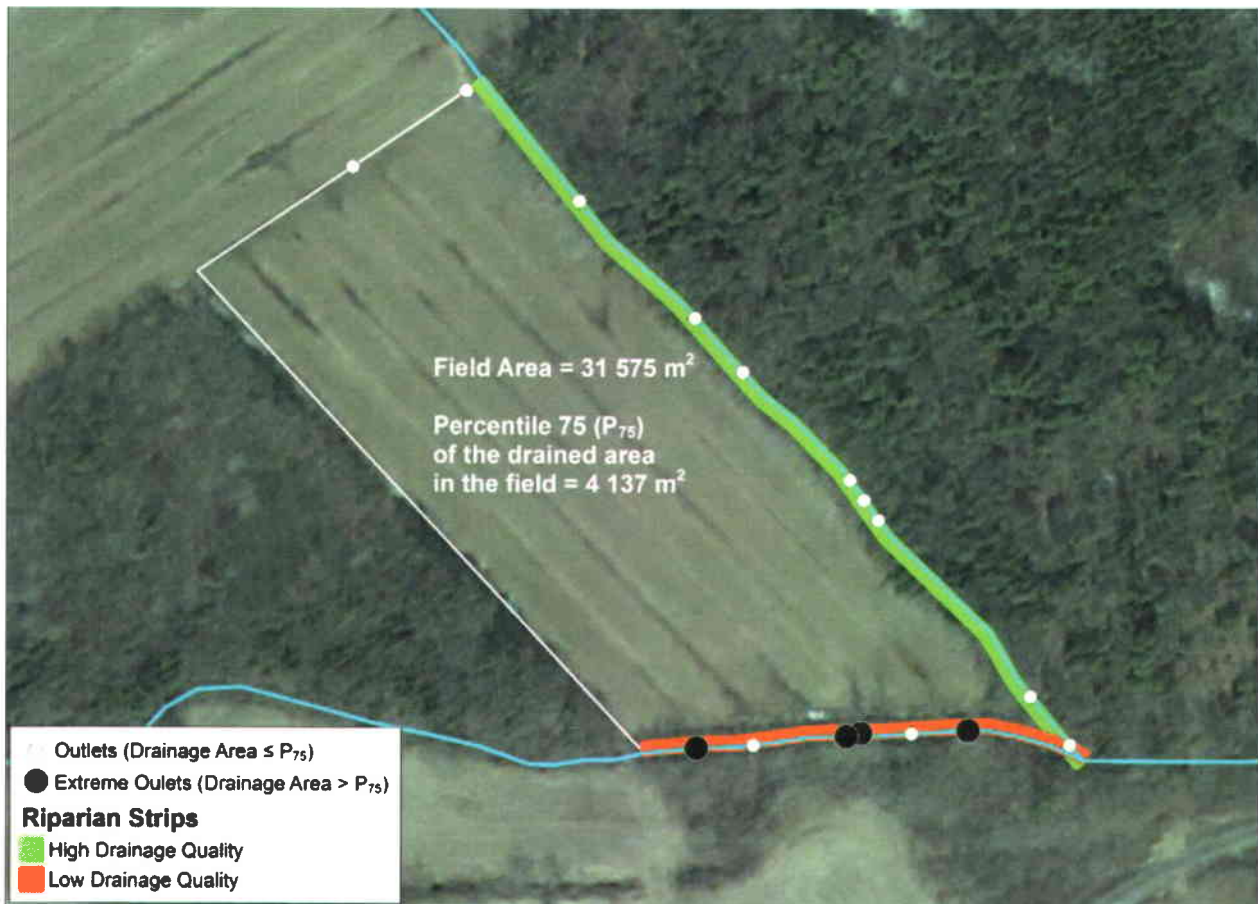
Figure 6.3 : Drainage configuration of an agricultural field.

Fig. 6.3 illustrates the drainage configuration of an agricultural field in the study area. The drainage points were classified as normal and extreme outlets. They were used to infer the potential amount of surface runoff volume in their locations inside the riparian strip. Extreme outlets were defined as those who have a cumulative surface runoff area greater than the 75th percentile (P_{75}). To illustrate this concept, first, all the outlets of the field (not only those inside a riparian strip) were sorted based on their drained area. Then, those with drained values greater than percentile 75 were classified as Extreme Outlets (black dots in Fig. 6.3). These points were used to theoretically depict areas where problems such as erosion rills, soil loss, and water pollution have the greatest potential to arise. Thus, the agricultural field in Fig. 6.3 has two riparian strips with different Drainage Quality (DQ). One with High DQ because it does not have extreme outlets inside it, which might indicate a fuzzy, constant water discharge, and one with Low DQ because all the extreme outlets of the field are inside its boundaries, with potentially-erosive surface runoff volumes.

66

This analysis was carried out individually for each riparian strip in the agricultural zone of the watershed. We did this in order to find relative extreme outlets, which enabled us to standardize the analysis, allowing for the wide variation in size among agricultural fields. In this context, drainage quality (DQ) must be considered as a relative measure of the performance of surface drainage in agricultural fields. The purpose of this metric is to detect whether the riverine strip is fulfilling its ecological functions based on the slope gradient (indirectly), and on the surface runoff streamflow. Anbumozhi *et al.* (2005) demonstrated that a riparian strip is more efficient at preventing concentrated flow erosion and capturing sediments and pollutants when it has a fuzzy drainage system, which is when flow discharge and velocity do not exceed critical values that enable the development of gullies or erosion rills.

6.2.8 Riparian Strip Efficiency Assessment in Agricultural Zones

Once the riparian strip quality index (IQBR) and the riparian strip drainage quality (DQ) were calculated, a categorization of both metrics was done, as follows:

Table 6.3: Categorization of the IQBR and the DQ

Category	IQBR	DQ
Very Low	< 40	> 0.75
Low	40 – 60	0.50 – 0.75
Moderate	60 – 80	0.25 – 0.50
High	> 80	< 0.25

The Riparian Strip Efficiency Index (RSEI) was then developed, combining the two previously calculated metrics into a categorical index that evaluates the quality of vegetation coverage and the quality of the hydrological configuration of the agricultural field in order to assess the fulfillment of its ecological functions. The RSEI, categorized as High, Moderate, Low, and Very Low, is calculated as follows:

$$RSEI = \min(IQBR, DQ)$$ (6.3)

6.3 Results and discussion

6.3.1 Object-based classification

The object-based classification performed well, achieving an overall coefficient kappa (K) of 0.82. As stated in previous sections, the composite raster file used for the classification was created by merging the first principal component and the NDVI of each image, reducing the spectral information, which speeded up processing time with minimal sacrifice of accuracy. This approach offers a simple, easily reproducible methodology that will enable land and environmental managers to gain a better understanding of riparian strips and their ecological roles in agricultural zones.

The 50-meter buffer zone used as the target area to extract riparian vegetation covered 15.1 km², which represents 13.7% of the whole river basin. Approximately 318 km of riverbanks were located within this geographic fence. *Forest* was the dominant class within the target area, covering 59.5% of the riparian zones. The second most important land cover class extracted was *Grass*, covering 32%. The remaining 8.5% corresponds to *Crops* (5.0%), *Infrastructure* (1.9%), *Herbaceous* (1.2%), *Bare Soil* (0.2%), and *Shrubs* (0.2%). Fig. 4 shows the spatial distribution of land cover inside riparian zones.
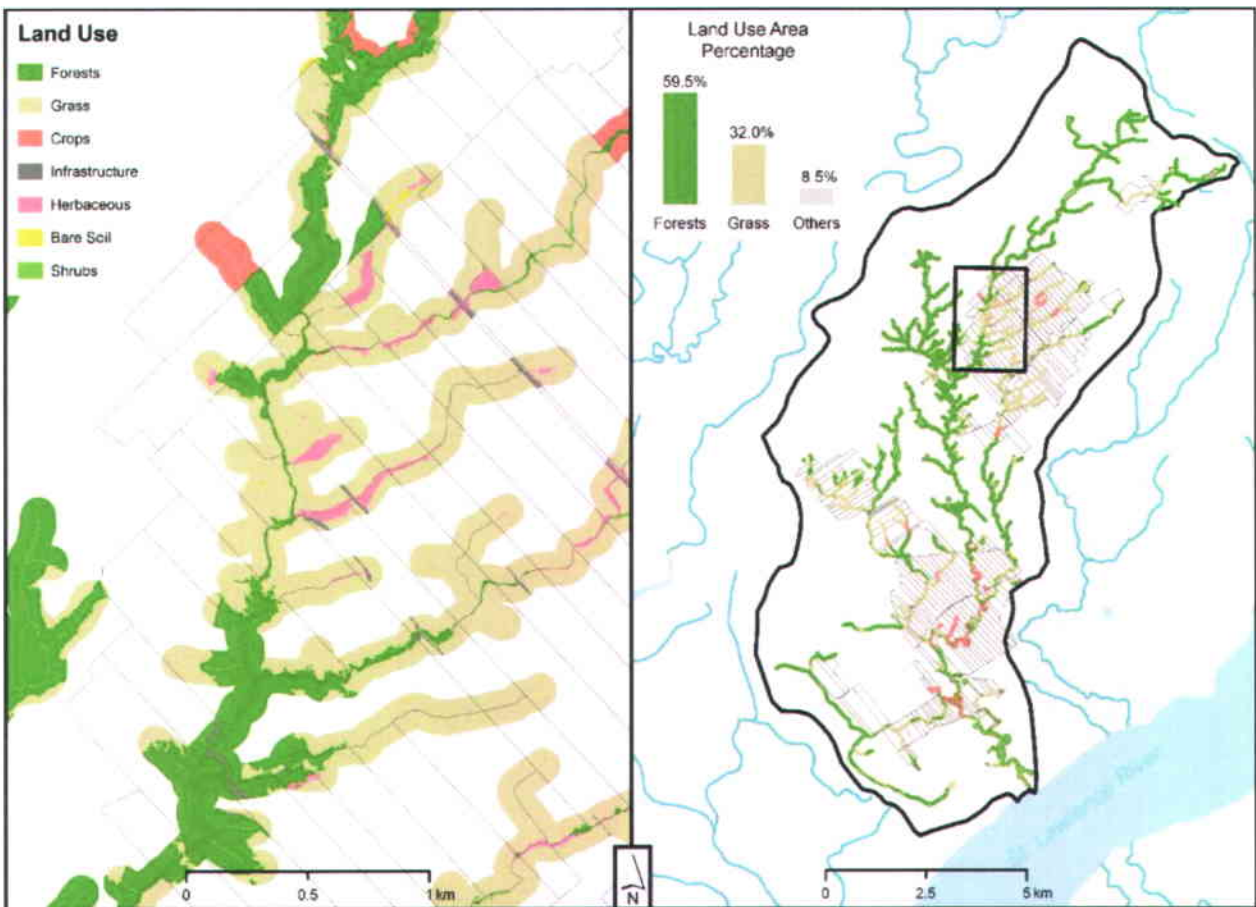
Figure 6.4 : On the left, land cover map of an agricultural zone near Saint-Gilbert. On the right, riparian zones' land cover map.

The La Chevrotière River is mostly surrounded by forests, but there are large zones of pasture and crops where the river passes through agricultural areas such as those at St-Gilbert or southeast of St-Marc-des-Carrières. It is inside these agricultural areas where most of the ecological problems are expected to occur, because of the constant human pressure on natural resources.

Once the land cover map was extracted, a validation sample size was estimated at 95% confidence level and with a margin of error of 10% (Congalton, 1991). Validation statistics were calculated using 181 samples selected randomly in proportion to the number of objects in each land cover class. Table 4 depicts the confusion matrix, showing the number of pixels classified into each land cover class against those selected in the validation process. The categories *Forests, Crops, Bare Soil,* and *Infrastructure* were the most accurate, showing the highest

agreement coefficients (K > 0.92), while *Shrubs, Herbaceous,* and *Grass* showed the lowest ones, ranging from 0.39 to 0.67.

Table 6.4: Confusion matrix from the object-based image classification.

Land cover Class	Reference Class (pixels)						
	(1)	(2)	(3)	(4)	(5)	(6)	(7)
(1) Forests	2,996,886	1,794	50,383	-	-	-	-
(2) Shrubs	2,611	5,253	5,751	-	-	-	-
(3) Herbaceous	1,683	2,702	36,510	-	-	-	-
(4) Crops	-	-	-	106,750	504,725	-	-
(5) Grass	2,124	-	282	-	1,726,520	-	-
(6) Bare Soil	-	-	-	-	-	7,659	-
(7) Infrastructure	1,005	-	-	-	-	623	99,777
K per Class	*0.99*	*0.54*	*0.39*	*1.00*	*0.67*	*0.92*	*1.00*
K	*0.82*						

Use of only the NDVI and the first principal component was not enough to accurately depict the low-performing classes. Their effect on the IQBR, and ultimately on the RSEI, is difficult to foresee with certainty, but the fact that they show confusion primarily against other types of natural vegetation is likely to reduce their effect on the indices, minimizing their negative impact. Refining techniques to improve the object-based classification might be envisaged in the future.

6.3.2 Riparian Strip Quality Assessment

Using the GIS analytical capabilities, each land cover area percentage was extracted from the classified map. Next, the IQBR was calculated for all riparian strips in the watershed. All riparian strips were divided every 500 meters, except in agricultural areas where they had the same length of the agricultural field they went through. The average ecological quality index in the river

basin was 69, which ranks it as a watershed with a moderate ecological quality. Most of the length of the riverbanks, 205.0 km (64%), was covered by riparian strips with a high IQBR; 36.9 km (12%) of the riverbanks were covered by riparian strips with a moderate IQBR, and 76.6 km (24%) were covered by riparian strips with a low or very low IQBR (Fig. 6.5).

It is noteworthy that in agricultural areas the ecological quality of riparian strips decreased considerably, presenting a mean IQBR of 56 (Low), 13 points lower than the overall watershed IQBR (Moderate). The value calculated for agricultural areas matches that calculated from the data collected during fieldwork (55), which could be seen as a demonstration of the usefulness of the proposed methodology, which can replicate the results of the in-situ methodology using less resources. In contrast, the mean IQBR of riparian strips located outside agricultural areas was 80 (High), which highlights the fact that most of the ecological problems of riparian strips are caused by anthropogenic activities.

When the IQBR over the whole watershed is compared to the IQBR in agricultural zones the proportion of riverbanks covered by riparian strips with a high IQBR decreases by more than half, from 64% to 29%, those with moderate IQBR remains stable, increasing in percentage only from 12% to 16%, and low and very low IQBR riparian strips increase in percentage by more than double, from 24% to 55%.
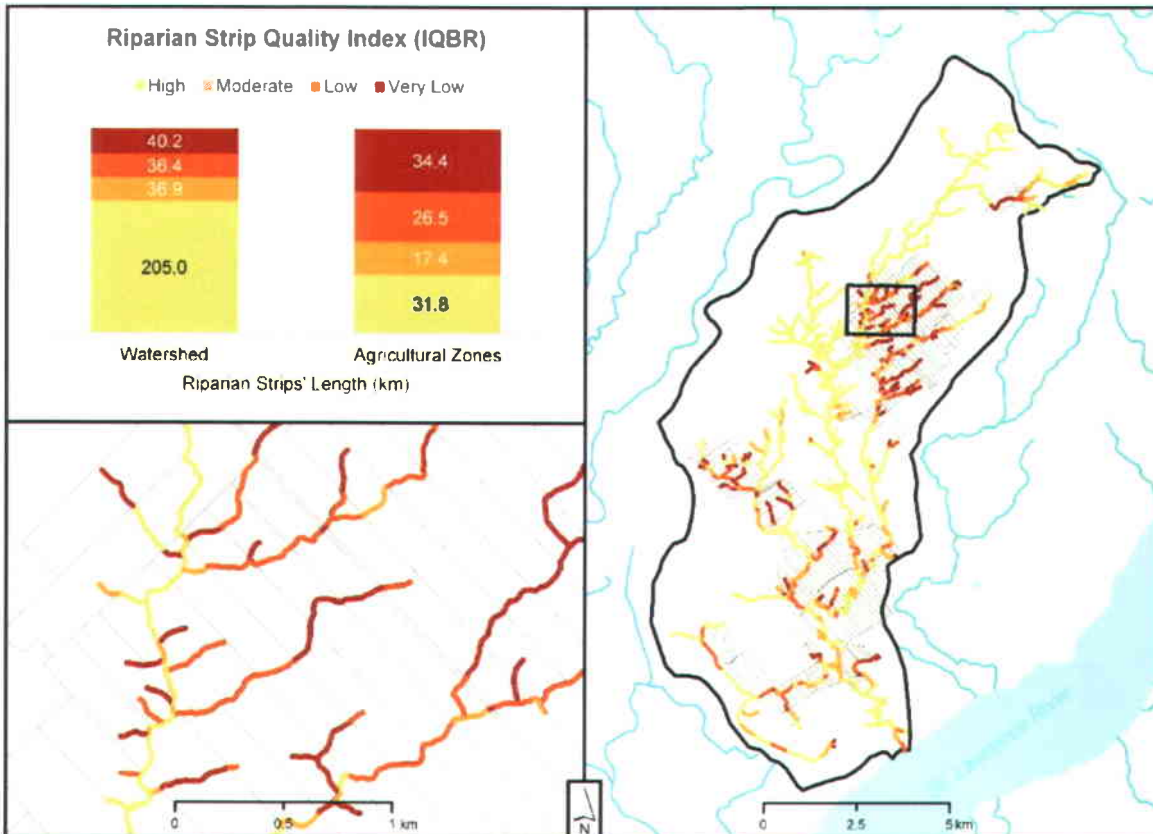
Figure 6.5 : Riparian strip quality index (IQBR) spatial distribution (right and bottom left) and comparison between the IQBR of the watershed and that of its agricultural zone (top left)

6.3.3 Riparian Strip Efficiency Assessment

The efficiency of riparian strips at filtering surface runoff and retaining sediments in agricultural zones was calculated by using hydrologic information such as potential propensity to generate surface runoff, in addition to the previously evaluated index of ecological quality (IQBR). These variables, which represent the hydrological connection of the agricultural field and the riparian strip, were extracted from the satellite-derived DEM and used to calculate the drainage quality (DQ) of each riparian strip (Eq. 6.2). Out of the approximately 110 km of riverbanks in agricultural areas, 65.1 km (59%) had a high DQ, 33.8 km (31%) had a moderate DQ, and 11.2 km (10%) had a low or very low DQ. The drainage configuration of agricultural land in this watershed seems therefore to be acceptable, but the DQ calculations indicate that there are 11.2 km of riverbanks with potential runoff concentration problems which might induce to soil

72

loss or water pollution (Fig. 6.6). In this way, the drainage quality metric can assist in detection of riverbanks negatively impacted by their upland drainage system, and to convey to land managers interesting insights about how the hydrologic configuration may influence filtering capacity of riparian strips.
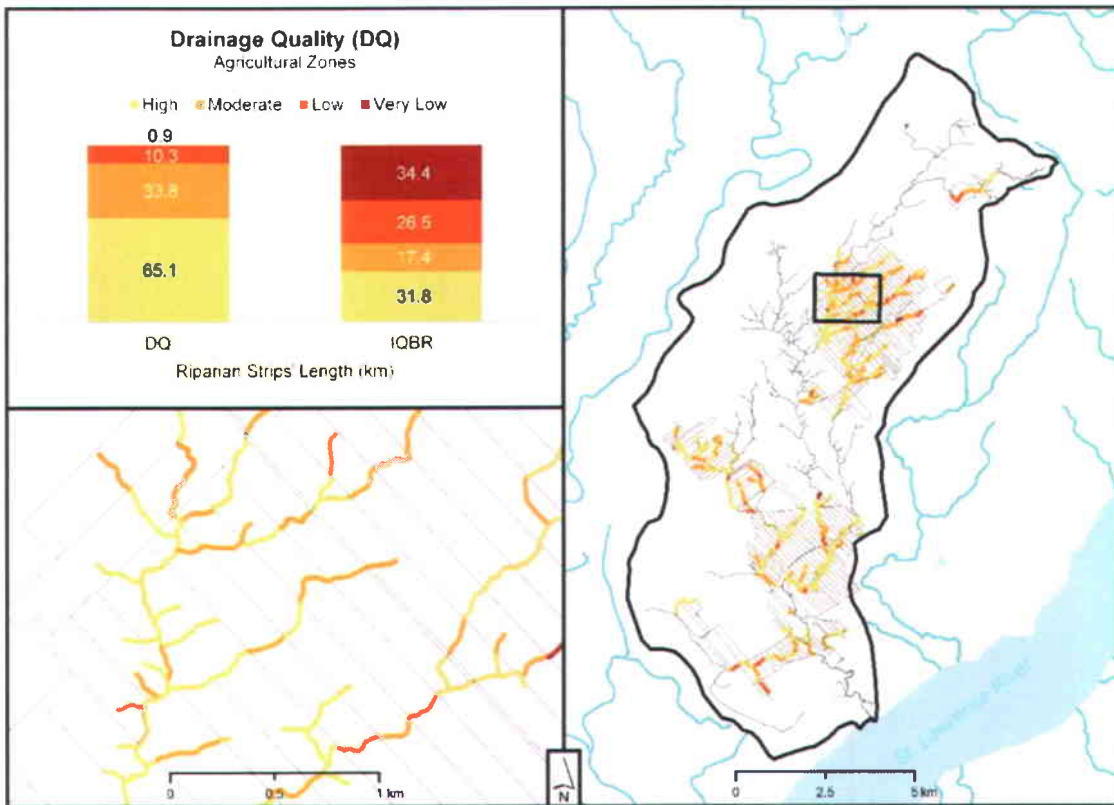

Figure 6.6 : Drainage Quality (DQ) spatial distribution in agricultural zones (right and bottom left), and summary data of the DQ and the IQBR (top left)

As detailed in Eq. 6.3, the IQBR and the DQ were combined to calculate the riparian strip efficiency index (RSEI). Each riparian strip crossing cropland was assigned either its IQBR or its DQ category, whichever was the lowest. As a consequence of the inclusion of the drainage quality metric, some riparian strips previously categorized as high quality (High IQBR) were downgraded to a Moderate or even to a Low or Very Low category. Figure 6.7 shows how the hydrologic configuration could be used to improve the discrimination and categorization of the potential ecological performance of riparian strips.

73
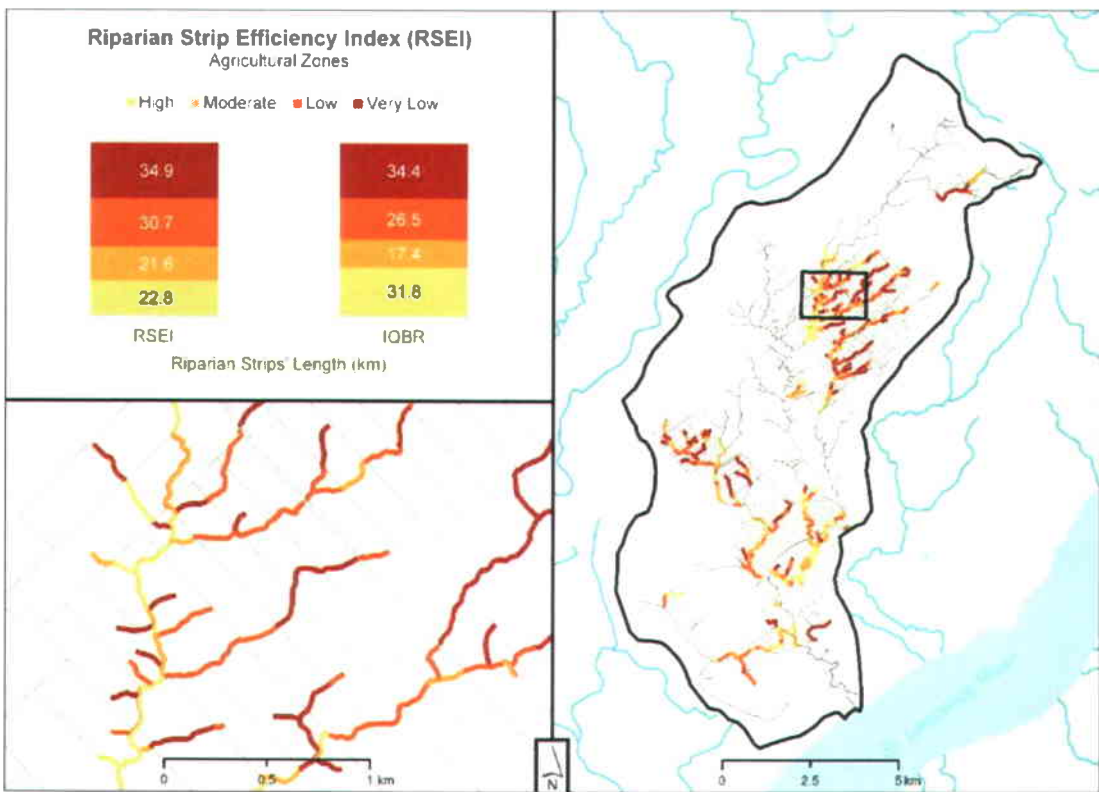
Figure 6.7 : Riparian Strip Efficiency Index spatial distribution (right and bottom left), and summary data of the IQBR and the RSEI in agricultural areas (top left).

New insights were revealed by using the RSEI as a substitute for the IQBR. Although 29% (31.8 km) of the riverbanks were classified with a High IQBR, only 21% (22.8 km) were assessed as highly efficient by the RSEI. This represents a difference of 9 km, a probably not insignificant amount when budgeting annual maintenance and mitigation plans in the watershed. The next two categories, Moderate and Low, increased from 16% (17.4 km) to 19% (21.6 km) and from 24% (26.5 km) to 28% (30.7 km), respectively. The lowest category in both indices remained almost the same. These changes in percentage distribution indicate that the IQBR overestimates the ecological capabilities of riverine zones. Thus, one might consider the RSEI more complete for discriminating the efficiency of riparian strips to fulfill their hydrological and ecological services.

6.4 Conclusions

The very high spatial resolution of stereoscopic imagery provided by the WorldView-2 satellite represents a suitable source of geospatial information for assessing the ecological quality and efficiency of riparian strips in low-relief watersheds. In this research, a spectrally simplified set of information was used to extract land cover information. Restricting the data to just the first principal component and the NDVI facilitated the process of object-based image analysis while still producing acceptable overall agreement (K = 0.82). However, there is plenty of potential scope for improving the accuracy of the land cover information extracted, especially if more spectral bands and vegetation ratios are included in the analysis, taking advantage of the new spectral bands available with this satellite. The satellite-derived DEM used to extract the hydrologic variables (positions of drainage outlets, and potential to concentrate surface runoff) was also found to be suitable for its task. As with the object-based image analysis, however, further improvements are possible: several other flow-routing algorithms are available that could be used to improve the accuracy of the hydrologic variables and thus improve the overall accuracy of riparian strip efficiency assessments.

Agricultural areas are placing increasing pressure on riparian habitats, causing ecological problems such as erosion and water pollution. The land cover and topographic information collected during the fieldwork for this research, mostly in agricultural areas, were used to estimate the riparian strip quality index (IQBR) for the various land cover areas within the study watershed. For agricultural areas, the on-site IQBR value was 55, corresponding to a *Low* ecological quality. The comparable figure calculated using the satellite-based methodology was 56, demonstrating the high degree of agreement between the two methodologies. As the latter is easier and less expensive to replicate on a regular basis, it is likely to be appealing to watershed management agencies. The improved ability to identify the most ecologically fragile riparian strips offered by this technique could lead to better environmental management practices and help land planners better allocate their efforts to mitigate the negative impacts occurring in these vulnerable areas.

Use of land cover information and hydrologic variables in conjunction enabled better discrimination and assessment of the most endangered riparian strips in an agricultural zone. The same methodology, with minor modifications, could be applied in other watersheds using

any very high spatial resolution geospatial information. With future improvements, this approach has the potential for wide application.

6.5 **Acknowledgements**

7 RÉFÉRENCES

Aarons & Gourley (2013) The role of riparian buffer management in reducing off-site impacts from grazed dairy systems. *Renew Agr Food Syst* 28(1):1-16.

Aguilar, Mills, Delgado, Aguilar, Negreiros & Perez (2010) Modelling vertical error in LiDAR-derived digital elevation models. *Isprs J Photogramm* 65(1):103-110.

Anbumozhi, Radhakrishnan & Yamaji (2005) Impact of riparian buffer zones on water quality. *Ecol Eng* 24(5):517-523.

Ashraf, Brabyn, Hicks & Collier (2010) Satellite remote sensing for mapping vegetation in New Zealand freshwater environments: A review. *New Zeal Geogr* 66(1):33-43.

ASPRS (2007) *Digital elevation model technologies and applications: the DEM users manual.* American Society for Photogrammetry & Remote Sensing,

Basnyat, Teeter, Lockaby & Flynn (2000) The use of remote sensing and GIS in watershed level analyses of non-point source pollution problems. *Forest Ecol Manag* 128(1-2):65-73.

Beaulieu, Breune & Guillou (2007) Avaloirs et puisards (Inlet and Drainage Wells). (Partenariat entre le ministère de l'Agriculture, des Pêcheries et de l'Alimentation du Québec et d'Agriculture et Agroalimentaire Canada, Quebec).

Benz, Hofmann, Willhauck, Lingenfelder & Heynen (2004) Multi-resolution, object-oriented fuzzy analysis of remote sensing data for GIS-ready information. *Isprs J Photogramm* 58(3-4):239-258.

Benz U, Baatz M & Schreier G (2001) OSCAR - Object oriented segmentation and classification of advanced radar allow automated information extraction. *Igarss 2001: Scanning the Present and Resolving the Future, Vols 1-7, Proceedings*:1913-1915.

Bereswill, Streloke & Schulz (2013) Current-use pesticides in stream water and suspended particles following runoff: Exposure, effects, and mitigation requirements. *Environ Toxicol Chem* 32(6):1254-1263.

Blaschke (2010) Object based image analysis for remote sensing. *Isprs J Photogramm* 65(1):2-16.

Borin, Passoni, Thiene & Tempesta (2010) Multiple functions of buffer strips in farming areas. *Eur J Agron* 32(1):103-111.

Boutin, Jobin & Belanger (2003) Importance of riparian habitats to flora conservation in farming landscapes of southern Quebec, Canada. *Agr Ecosyst Environ* 94(1):73-87.

Burrough (1986) *Principles of geographical information systems for land resources assessment.* Clarendon Press, Oxford. xiii, 194 p., [194] p. de planches p

Büyüksalih, Baz, Alkan & Jacobsen (2012) DEM Generation with WorldView-2 Images. in *XXII ISPRS Congress* (International Archives of the Photogrammetry, Remote Sensing and Spatial Information Science, Melbourne, Australia).

Callow, Niel V & Boggs (2007) How does modifying a DEM to reflect known hydrology affect subsequent terrain analysis? *J Hydrol* 332(1-2):30-39.

CAPSA (2011) Portrait préliminaire des nouvelles zones de gestion intégrée de l'eau par bassin versant de la CAPSA : les bassins versants des rivières La Chevrotière et Belle-Isle. (Organisme des bassins versants des rivières Sainte-Anne, Portneuf, La Chevrotière et Belle-Isle, St-Raymmond, Québec).

Congalton (1991) A review of assessing the accuracy of classifications of remotely sensed data. *Remote Sens Environ* 37(1):35-46.

Congalton, Birch, Jones & Schriever (2002) Evaluating remotely sensed techniques for mapping riparian vegetation. *Comput Electron Agr* 37(1-3):113-126.

Chaplot, Darboux, Bourennane, Leguedois, Silvera & Phachomphon (2006) Accuracy of interpolation techniques for the derivation of digital elevation models in relation to landform types and data density. *Geomorphology* 77(1-2):126-141.

Charrier & Li (2012) Assessing resolution and source effects of digital elevation models on automated floodplain delineation: A case study from the Camp Creek Watershed, Missouri. *Appl Geogr* 34:38-46.

Charron, Lalonde, Roy, Boyer & Turgeon (2008) Changes in riparian habitats along five major tributaries of the Saint Lawrence River, Quebec, Canada: 1964-1997. *River Res Appl* 24(5):617-631.

Chaubey, Cotter, Costello & Soerens (2005) Effect of DEM data resolution on SWAT output uncertainty. *Hydrol Process* 19(3):621-628.

Chauvette L (2006) Portrait globale de l'état des berges et bandes riveraines du tronçon principal de la rivière Béncancour. (Groupe de concertation du bassin de la rivière Bécancour (GROBEC)).

DeVenecia, Walker & Zhang (2007) New approaches to generating and processing high resolution elevation data with imagery. *Photogrammetric Week* (200).

Dragut, Tiede & Levick (2010) ESP: a tool to estimate scale parameter for multiresolution image segmentation of remotely sensed data. *Int J Geogr Inf Sci* 24(6):859-871.

Duchemin & Hogue (2009) Reduction in agricultural non-point source pollution in the first year following establishment of an integrated grass/tree filter strip system in southern Quebec(Canada). *Agr Ecosyst Environ* 131(1-2):85-97.

Duchemin & Majdoub (2004) Les bandes végétales filtrantes: de la parcelle au bassin versant. in *VECTEUR ENVIRONNEMENT* (Institut de recherche et de développement en agroenvironnement (IRDA)), p 15.

Eckert, Kellenberger & Itten (2005) Accuracy assessment of automatically derived digital elevation models from aster data in mountainous terrain. *Int J Remote Sens* 26(9):1943-1957.

Endreny & Wood (2001) Representing elevation uncertainty in runoff modelling and flowpath mapping. *Hydrol Process* 15(12):2223-2236.

Erskine, Green, Ramirez & MacDonald (2007) Digital elevation accuracy and grid cell size: Effects on estimated terrain attributes. *Soil Sci Soc Am J* 71(4):1371-1380.

Fernandez, Barquin, Alvarez-Cabria & Penas (2012) Quantifying the performance of automated GIS-based geomorphological approaches for riparian zone delineation using digital elevation models. *Hydrol Earth Syst Sc* 16(10):3851-3862.

Fortier, Gagnon, Truax & Lambert (2010) Nutrient accumulation and carbon sequestration in 6-year-old hybrid poplars in multiclonal agricultural riparian buffer strips. *Agr Ecosyst Environ* 137(3-4):276-287.

Ge, Thomasson & Sui (2011) Remote sensing of soil properties in precision agriculture: A review. *Front Earth Sci-Prc* 5(3):229-238.

Gergel, Stange, Coops, Johansen & Kirby (2007) What is the value of a good map ? An example using high spatial resolution imagery to aid riparian restoration. *Ecosystems* 10(5):688-702.

Ghosh & Joshi (2014) A comparison of selected classification algorithms for mapping bamboo patches in lower Gangetic plains using very high resolution WorldView 2 imagery. *Int J Appl Earth Obs* 26(0):298-311.

Goetz (2006) Remote sensing of riparian buffers: Past progress and future prospects (vol 1, pg 133, 2006). *J Am Water Resour As* 42(3):806-806.

Goetz, Wright, Smith, Zinecker & Schaub (2003) IKONOS imagery for resource management: Tree cover, impervious surfaces, and riparian buffer analyses in the mid-Atlantic region. *Remote Sens Environ* 88(1-2):195-208.

Gu & Liu (2010) Applications of remote sensing and GIS to the assessment of riparian zones for environmental restoration in agricultural watersheds. *Geo-spatial Information Science* 13(4):263-268.

Gumiere, Bissonnais L, Raclot & Cheviron (2011) Vegetated filter effects on sedimentological connectivity of agricultural catchments in erosion modelling: a review. *Earth Surf Proc Land* 36(1):3-19.

Guo, Li, Yu & Alvarez (2010) Effects of topographic variability and Lidar sampling density on several DEM interpolation methods. *Photogramm Eng Rem S* 76(6):701-712.

Hage E, Simonetto, Faour & Polidori (2012) Evaluation of elevation, slope and stream network quality of SPOT DEMs. in *XXII ISPRS Congress* (International Archives of the Photogrammetry, Remote Sensing and Spatial Information Science, Melbourne, Australia).

Hay, Castilla, Wulder & Ruiz (2005) An automated object-based approach for the multiscale image segmentation of forest scenes. *Int J Appl Earth Obs* 7(4):339-359.

Hellweger (1997) AGREE - DEM surface reconditioning system. (University of Texas at Austin, Austin, TX).

Hickey & Doran (2004) A review of the efficiency of buffer strips for the maintenance and enhancement of riparian ecosystems. *Water Qual Res J Can* 39(3):311-317.

Hobi & Ginzler (2012) Accuracy assessment of digital surface models based on WorldView-2 and ADS80 stereo remote sensing data. *Sensors-Basel* 12(5):6347-6368.

Hohle & Hohle (2009) Accuracy assessment of digital elevation models by means of robust statistical methods. *Isprs J Photogramm* 64(4):398-406.

Hosl, Strauss & Glade (2012) Man-made linear flow paths at catchment scale: Identification, factors and consequences for the efficiency of vegetated filter strips. *Landscape Urban Plan* 104(2):245-252.

Hosseinzadeh (2011) Assessing the quality of ASTER DEMs for Hydrological Applications. in *2011 International Conference on Environment Science and Engineering* (IPCBEE, Singapore).

Huaxing (2008) Modelling Terrain Complexity. *Lecture Notes in Geoinformation and Cartography: Advances in Digital Terrain Analysis*, Qiming Zhou BL, Guo-an Tang (Édit.) Springer-Verlag, Berlin. p 1 texte ©*lectronique.

Hupp & Osterkamp (1996) Riparian vegetation and fluvial geomorphic processes. *Geomorphology* 14(4):277-295.

Jacobsen (2004) DEM generation from satellite data. *Remote Sensing in Transition*:513-525.

Janisch, Wondzell & Ehinger (2012) Headwater stream temperature: Interpreting response after logging, with and without riparian buffers, Washington, USA. *Forest Ecol Manag* 270:302-313.

Jenson & Domingue (1988a) Extracting topographic structure from digital elevation data for geographic information system analysis. *Photogramm Eng Rem S* 54(11):1593-1600.

Jenson SK & Domingue JO (1988b) Extracting Topographic Structure from Digital Elevation Data for Geographic Information-System Analysis. *Photogramm Eng Rem S* 54(11):1593-1600.

Johansen, Arroyo, Phinn & Witte (2010) Comparison of geo-object based and pixel-based change detection of riparian environments using high spatial resolution multi-spectral imagery. *Photogramm Eng Rem S* 76(2):123-136.

Johansen, Coops, Gergel & Stange (2007) Application of high spatial resolution satellite imagery for riparian and forest ecosystem classification. *Remote Sens Environ* 110(1):29-44.

Jones KB, Slonecker ET, Nash MS, Neale AC, Wade TG & Hamann S (2010) Riparian habitat changes across the continental United States (1972-2003) and potential implications for sustaining ecosystem services. *Landscape Ecol* 25(8):1261-1275.

Kenward, Lettenmaier, Wood & Fielding (2000) Effects of digital elevation model accuracy on hydrologic predictions. *Remote Sens Environ* 74(3):432-444.

Li, Gold & Zhu (2005) *Digital terrain modeling principles and methodology.* CRC Press, New York. xvi, 323 p. p. http://www.myilibrary.com?id=21630

Li, Shi, Li, Muller, Drummond, Li, Li, Li & Liu (2012) Evaluation of ASTER GDEM v2 using GPS measurements and SRTM V4.1 in China. in *XXII ISPRS Congress* (ISPRS Annals of the Photogrammetry, Remote Sensing and Spatial Information Sciences, Melbourne, Australia).

Lin-Lin & Hong-Bin (2010) Impact of digital elevation model resolution on stream network parameters. in *2010 2nd Conference on Environmental Science and Information Application Technology* (IEEE, Wuhan, China).

Lin, Chou & Lin (2002) Modeling the width and placement of riparian vegetated buffer strips: a case study on the Chi-Jia-Wang Stream, Taiwan. *J Environ Manage* 66(3):269-280.

Lippitt, Coulter, Freeman, Lamantia-Bishop, Pang & Stow (2012) The effect of input data transformations on object-based image analysis. *Remote Sens Lett* 3(1):21-29.

Liu, Bian, Meng, Wang, Zhang, Yang, Shao & Wang (2012a) Discrepancy measures for selecting optimal combination of parameter values in object-based image analysis. *Isprs J Photogramm* 68:144-156.

Liu, Hu, Hu & Sherba (2012b) Approximation theory applied to DEM vertical accuracy assessment. *T Gis* 16(3):397-410.

Liu, Mang & Zhang (2008) Major factors influencing the efficacy of vegetated buffers on sediment trapping: A review and analysis. *J Environ Qual* 37(5):1667-1674.

Longley (2005) *Geographical information systems and science.* John Wiley & Sons, Chichester ; Etobicoke, Ont., 2nd. xvii, 517 p. p

Lowrance, Altier, Newbold, Schnabel, Groffman, Denver, Correll, Gilliam, Robinson, Brinsfield, Staver, Lucas & Todd (1997) Water quality functions of Riparian forest buffers in Chesapeake Bay watersheds. *Environ Manage* 21(5):687-712.

Lyon, Ward, Atheron, Senay & Krill (2003) Remote Sensing and GIS for Site-Specific Farming. *GIS for water resources and watershed management,* Lyon JG (Édit.) Taylor & Francis, London. p vii, 266 p., [216] p. de pl.

Maidment (2003) *Arc hydro : GIS for water resources.* ESRI Press, Redlands, Calif., 3rd print., June 2003. x, 203 p. p

MDDEFP (2002) Politique nationale de l'eau. (Gazzete Officielle du Québec, Québec).

MDDEFP (2005) Politique de protection des rives, du littoral et des plaines inondables. (Gazzete Officielle du Québec, Québec).

MDDEFP (2008) Indice de qualité de la bande riveraine (IQBR). (Ministère de Développement Durable, Environnement, Faune et Parcs, Québec).

Mitchel & MacNabb (2010) High resolution stereo satellite elevation mapping accuracy assessment. in *ASPRS 2010 Annual Conference* (American Society for Photogrammetry and Remote Sensing, San Diego, California), p 12.

Moore, Grayson & Ladson (1991) Digital terrain modeling - a review of hydrological, geomorphological, and biological Applications. *Hydrol Process* 5(1):3-30.

Mukherjee, Mukherjee, Garg, Bhardwaj & Raju (2013) Evaluation of topographic index in relation to terrain roughness and DEM grid spacing. *J Earth Syst Sci* 122(3):869-886.

Muller, Decamps & Dobson (1993) Contribution of space remote sensing to river studies. *Freshwater Biol* 29(2):301-312.

Mutanga, Adam & Cho (2012) High density biomass estimation for wetland vegetation using WorldView-2 imagery and random forest regression algorithm. *Int J Appl Earth Obs* 18:399-406.

Naiman & Decamps (1997) The ecology of interfaces: Riparian zones. *Annu Rev Ecol Syst* 28:621-658.

Nardi, Grimaldi, Santini, Petroselli & Ubertini (2008) Hydrogeomorphic properties of simulated drainage patterns using digital elevation models: the flat area issue. *Hydrolog Sci J* 53(6):1176-1193.

Narumalani, Zhou & Jensen (1997) Application of remote sensing and geographic information systems to the delineation and analysis of riparian buffer zones. *Aquat Bot* 58(3-4):393-409.

NDEP (2004) Guidelines for digital elevation data. Version 1.0. National Digital Elevation Program. Édit Infrastructure NSD).

Nigel & Rughooputh (2010a) Mapping of monthly soil erosion risk of mainland Mauritius and its aggregation with delineated basins. *Geomorphology* 114(3):101-114.

Nigel R & Rughooputh SDDV (2010b) Soil erosion risk mapping with new datasets: An improved identification and prioritisation of high erosion risk areas. *CATENA* 82(3):191–205.

Nigel R & Rughooputh SDDV (2013) Application of a RUSLE-based soil erosion modelling on Mauritius Island. *Soil Research* 50(8):645–651.

Novoa, Chokmani, Nigel & Dufour (2013) Quality assessment from a hydrologic perspective of a digital elevation model derived from WorldView-2 remote sensing data. *Hydrolog Sci J* DOI: 10.1080/02626667.2013.875179.

Parn, Pinay & Mander (2012) Indicators of nutrients transport from agricultural catchments under temperate climate: A review. *Ecol Indic* 22:4-15.

Piechnik, Goslee, Veith, Bishop & Brooks (2012) Topographic placement of management practices in riparian zones to reduce water quality impacts from pastures. *Landscape Ecol* 27(9):1307-1319.

Québec Gd (2005) Politique de protection des rives, du littoral et des plaines inondables. *Gazette officielle du Québec*:2180-2191.

Reinartz, d'Angelo, Krauß, Poli, Jacobsen & Buyuksalih (2010) Benchmarking and quality analysis of dem generated from high and very high resolution optical stereo satellite data". in *ISPRS Symp. Commission I, Int. Archives*

Photogrammetry, Remote Sensing and Spatial Information Sciences, vol. *XXXVIII* (Convergence in Geomatics, CGC, ISPRS).

Rezak, Laborde & Errih (2012) Validation of a digital terrain model suitable for regional hydrological modelling in northern Algeria. *Hydrolog Sci J* 57(5):928-941.

Richter (1997) Correction of atmospheric and topographic effects for high spatial resolution satellite imagery. *Int J Remote Sens* 18(5):1099-1111.

Sahu & Gu (2009) Modeling the effects of riparian buffer zone and contour strips on stream water quality. *Ecol Eng* 35(8):1167-1177.

Saint-Jacques & Richard (1998) Développement d'un indice de qualité de la bande riveraine: application à la rivière Chaudière et mise en relation avec l'intégrité biotique du milieu acuatique. *Ministère de l'Environnement et de la Faune (éd.)* (Le bassin versant de la rivière Chaudière: l'état de l'écosystème acuatique - 1996):6.1 à 6.41.

Shore, Murphy, Jordan, Mellander, Kelly-Quinn, Cushen, Mechan, Shine & Melland (2013) Evaluation of a surface hydrological connectivity index in agricultural catchments. *Environ Modell Softw* 47:7-15.

Teufl, Weigelhofer, Fuchsberger & Hein (2013) Effects of hydromorphology and riparian vegetation on the sediment quality of agricultural low-order streams: consequences for stream restoration. *Environ Sci Pollut R* 20(3):1781-1793.

Tormos, Kosuth, Durrieu, Villeneuve & Wasson (2011) Improving the quantification of land cover pressure on stream ecological status at the riparian scale using High Spatial Resolution Imagery. *Phys Chem Earth* 36(12):549-559.

Toutin & Cheng (2002) Comparison of automated digital elevation model extraction results using along-track ASTER and across-track SPOT stereo images. *Opt Eng* 41(9):2102-2106.

Trimble (2011) eCognition Developer 8.6: User's Guide. (Trimble Germany GmbH, München, Germany).

Vaaja, Hyyppa, Kukko, Kaartinen, Hyyppa & Alho (2011) Mapping topography changes and elevation accuracies using a mobile laser scanner. *Remote Sens-Basel* 3(3):587-600.

Vaze, Teng & Spencer (2010) Impact of DEM accuracy and resolution on topographic indices. *Environ Modell Softw* 25(10):1086-1098.

Velde vd, Rozemeijer, Rooij d, Geer v & Broers (2010) Field-scale measurements for separation of catchment discharge into flow route contributions. *Vadose Zone J* 9(1):25-35.

Vézina A, Savoie C, Desmarais C, Lemieux N, Cloutier L-M & Dion J-P (2003) Utilisation de l'imagerie numérique infrarouge pour évaluer la performance agroenvironnementale d'entreprises agricoles. (Fonds d'action québécois pour le développement durable, Québec, Canada), p 17.

Vought, Pinay, Fuglsang & Ruffinoni (1995) Structure and function of buffer strips from a water-quality perspective in agricultural landscapes. *Landscape Urban Plan* 31(1-3):323-331.

Wechsler SP (2007) Uncertainties associated with digital elevation models for hydrologic applications: a review. *Hydrology and Earth System Sciences* 11:1481–1500.

Wilson (2012) Digital terrain modeling. *Geomorphology* 137(1):107-121.

Wilson, Aggett, Yongxin & Lam (2008) Water in the Landscape: A Review of Contemporary Flow Routing Algorithms. *Advances in Digital Terrain Analysis,* (Lecture Notes in Geoinformation and Cartography, Zhou Q, Lees B & Tang G-A (Édit.) Springer Berlin Heidelberg, 10.1007/978-3-540-77800-4_12. p 213-236.

Wilson, Lam & Deng (2007) Comparison of the performance of flow-routing algorithms used in GIS-based hydrologic analysis. *Hydrol Process* 21(8):1026-1044.

Wise (2000) Assessing the quality for hydrological applications of digital elevation models derived from contours. *Hydrol Process* 14(11-12):1909-1929.

Wolock & Price (1994) Effects of digital elevation model map scale and data resolution on a topography-based watershed model. *Water Resour Res* 30(11):3041-3052.

Wu, Li & Huang (2008) A study on DEM-derived primary topographic attributes for hydrologic applications: Sensitivity to elevation data resolution. *Appl Geogr* 28(3):210-223.

Yang (2007a) Integrated use of remote sensing and geographic information systems in riparian vegetation delineation and mapping. *Int J Remote Sens* 28(1-2):353-370.

Yang X (2007b) Integrated use of remote sensing and geographic information systems in riparian vegetation delineation and mapping. *Int J Remote Sens* 28(1-2):353-370.

Zhang (2002) A new automatic approach for effectively fusing Landsat 7 as well as IKONOS images. *International Geoscience and Remote Sensing Symposium and 24th Canadian Symposium on Remote Sensing* I-VI:2429-2431.

Zhang, Drake, Wainwright & Mulligan (1999) Comparison of slope estimates from low resolution DEMs: Scaling issues and a fractal method for their solution. *Earth Surf Proc Land* 24(9):763-779.

Zhang, Li, Gong, Li, Song & Huang (2010) Hydrologic information extraction based on ArcHydro tool and DEM. *2010 International Conference on Challenges in Environmental Science and Computer Engineering.* (Wuhan, China, 7 March 2010) Institute of Electrical and Electronics Engineers (IEEE).

Zhang & Montgomery (1994) Digital elevation model grid size, landscape representation, and hydrologic simulations. *Water Resour Res* 30(4):1019-1028.

Zhou & Liu (2002) Error assessment of grid-based flow routing algorithms used in hydrological models. *Int J Geogr Inf Sci* 16(8):819-842.

Zhou & Liu (2004) Error analysis on grid-based slope and aspect algorithms. *Photogramm Eng Rem S* 70(8):957-962.